



Contents lists available at SciVerse ScienceDirect

Journal of Volcanology and Geothermal Research

journal homepage: www.elsevier.com/locate/jvolgeores

Observations of volcanic lightning during the 2009 eruption of Redoubt Volcano

Sonja A. Behnke^{a,*}, Ronald J. Thomas^a, Stephen R. McNutt^b, David J. Schneider^c, Paul R. Krehbiel^a, William Rison^a, Harald E. Edens^a^a Langmuir Laboratory, New Mexico Tech, 801 Leroy Place, Socorro, NM 87801 USA^b Alaska Volcano Observatory, University of Alaska Fairbanks, 903 Koyukuk, Fairbanks, AK 99775 USA^c Alaska Volcano Observatory, United States Geological Survey, 4200 University Drive, Anchorage, AK 99508 USA

ARTICLE INFO

Article history:

Received 1 June 2011

Accepted 21 December 2011

Available online xxx

Keywords:

Volcanic lightning

Redoubt

Explosive Volcanism

VHF Lightning Mapping

ABSTRACT

Observations of volcanic lightning during the eruption of Redoubt Volcano in March and April 2009 were made with the Lightning Mapping Array. During the eruption twenty-three distinct episodes of volcanic lightning were observed. Electrical activity occurred as either a volcanic lightning storm with up to thousands of lightning discharges or as a weak electrical event with only a handful of lightning discharges. During the volcanic lightning storms we observed two phases of electrical activity: the explosive phase and the plume phase. The explosive phase consisted of very small discharges (on the order of 10–100 m) occurring directly above the vent while an explosive eruption was ongoing, whereas the plume phase was comprised of discharges occurring throughout the plume subsequent to the explosive eruption. The area of discharges during the explosive phase ranged from less than 1 km² to 50 km² or more. The electrical activity at the beginning of the plume phase was dominated by small discharges. Over time the horizontal extent of the flashes increased, with the largest flashes occurring at the end of the plume phase. The distribution of the horizontal size of the discharges over the lifetime of the storm indicate that the charge structure of the plume evolved from a complex and ‘clumpy’ structure to a more simple horizontally stratified structure. Plume height was shown to be a key factor in the quantity of lightning in a storm. The volcanic lightning storms occurred in plumes with column heights greater than 10 km. The tall plumes may contribute to the efficiency of charge generation through ice collisions by providing strong updrafts from the large thermal energy input from the eruption.

© 2011 Elsevier B.V. All rights reserved.

1. Introduction

Lightning is an inherent feature of many types of volcanic eruptions (McNutt and Williams, 2010), but it is not well understood how the characteristics of an eruption (e.g., plume height, temperature, magma composition, ash or gas content) influence the resulting electrical activity. The relationships between lightning and eruptive activity have recently been explored by some researchers (Hoblitt, 1994; McNutt and Davis, 2000; Bennett et al., 2010) using instruments that primarily detect the signals from cloud-to-ground lightning, while others (Thomas et al., 2010) have used methods that look at all the electrical activity in a plume including cloud-to-ground and intracloud lightning. Observations of so-called ‘total lightning’ are possible with the Lightning Mapping Array (LMA) (Rison et al., 1999; Thomas et al., 2004), which locates sources of VHF radiation that are produced from lightning as it propagates. The LMA effectively provides a map of all of the electrical activity in a plume, making detailed studies of volcanic lightning and its relationships to eruptive activity possible.

The LMA was previously used to study lightning during the 2006 eruption of Augustine Volcano, also in Alaska, which characterized the styles and types of electrical activity that occurred as a result of the eruption (Thomas et al., 2007; Thomas et al., 2010). One of the main results of the Augustine Volcano study was that lightning occurred in two distinct phases, an explosive phase and a plume phase. The explosive phase described electrical activity observed during the actual explosive event, while the plume phase described lightning that occurred in the plume subsequent to the explosive eruption. Additionally, lightning during the Augustine Volcano eruption was classified into three categories: vent discharges (small, 10–100 m, high rate discharges close to the vent), near-vent lightning (medium sized, 1–7 km discharges extending from the volcano into the eruption cloud) and plume lightning (large sized, 10 km or more, branched discharges similar to intracloud (IC) lightning observed in thunderstorms).

More recently, the LMA was used to study lightning during the eruption of Redoubt Volcano, located in south-central Alaska (Fig. 1). Redoubt Volcano underwent a series of explosive eruptions in late March and early April of 2009, most of which produced substantial electrical activity. The major events occurred between 23 March and 4 April, 2009, though the full period of explosive activity extended through April 5. Peak plume heights for each explosive event ranged from 5 to 19 km, and the entire eruption was classified

* Corresponding author.

E-mail address: sbehnke@nmt.edu (S.A. Behnke).

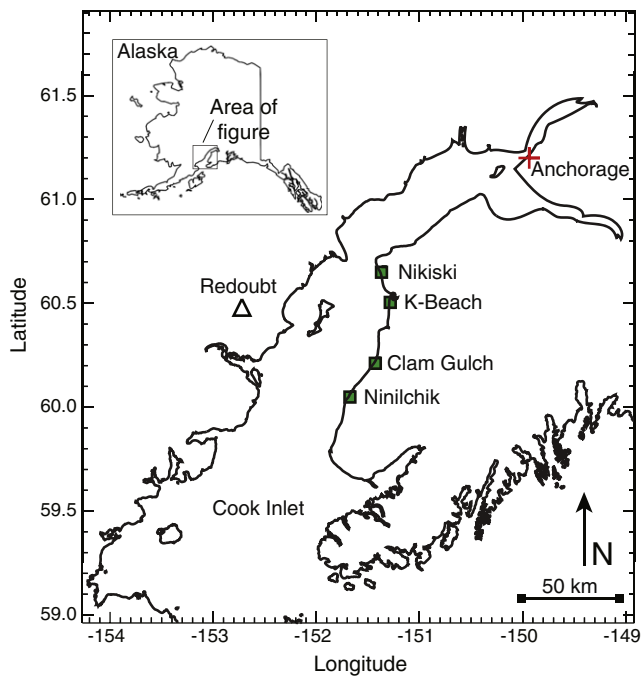


Fig. 1. Map of the locations of the lightning mapping stations (squares) and Redoubt Volcano (triangle).

as a VEI 3 event (Schaefer, 2011). A 4-station LMA was deployed on the east side of Cook Inlet about two months before the eruption to study the electrical activity of the volcano. During the two week period of explosive activity, the ash plumes from Redoubt Volcano produced prolific lightning, which was recorded by the LMA, though visual observations were scarce due to inclement weather in the area.

The research presented in this article expands on the Augustine Volcano results and shows the relationship between the eruptive and electrical activity at Redoubt Volcano in an effort to understand what lightning can tell us about a volcanic eruption. We present an overview of the electrical activity that occurred during the eruptive events and compare it to the previous observations from Augustine Volcano. The trends observed in the progression of flash rate and flash area over time are shown and the types of lightning discharges that occurred throughout the eruption column are discussed. Finally, the electrical activity is compared to the peak plume heights and the seismic and acoustic signals from each explosive event.

2. Data and methods

This study used lightning data from the New Mexico Tech Lightning Mapping Array, seismic, acoustic, and radar data from the Alaska Volcano Observatory, and measurements of cloud-to-ground lightning from the Alaska BLM and the World Wide Lightning Location Network.

2.1. The Lightning Mapping Array

Four LMA stations were installed on the Kenai Peninsula, approximately 80 km east of Redoubt Volcano, between 28 and 31 January 2009. Station sites were selected based on access to AC power and broadband internet, on having a line-of-sight view to Redoubt Volcano, and on being a radio frequency (RF) quiet location. The internet, line of sight, and noise constraints greatly limited the number of desirable sites, so the authors made use of the best locations available. A map of the station locations is shown in Fig. 1. Although each station had a line-of-sight view to Redoubt Volcano, the actual vent of the volcano was blocked from view at the stations because there was a ridge on

the eastern side of the volcano that extended approximately 600 m above the vent. This prevented any electrical signals that occurred below and behind the ridge from reaching the stations.

The LMA uses time-of-arrival methods (Rison et al., 1999) to locate sources of VHF radiation (typically 63 MHz; in this deployment 63 and 57 MHz were used) that are produced during the development of lightning channels. In successive short time windows (10 or 80 μ s, depending on the operating mode), the peak amplitude and arrival time of the received power is recorded if the signal exceeds a local noise threshold. The LMA was operating in 10 μ s mode during the Redoubt Volcano deployment. Each station uses timing from a GPS receiver to measure the arrival times with an accuracy of 40–50 ns. Each electrical signal recorded by the LMA represents a small piece of a discharge, and hundreds or thousands of signals may be recorded for one lightning discharge, depending on the size of a discharge. A minimum of four stations is needed to determine the three dimensional location and time of the source event.

An example of the data recorded by an LMA station is shown in Fig. 2. In each of these three plots, the colors indicate the relative density of points, purple being least dense and red most dense. Panel (a) shows the peak power received in each 10 μ s time window. The bands of background radiation (the steady purple sources between roughly -80 and -70 dBm and the greenish sources below -80 dBm) throughout the plot are caused by local noise sources such as electronics, motors, or transformers. A discrete vertical line on a plot of this time scale is most likely caused by a lightning discharge, but can also be produced by a strong, discrete noise source. Panel (b) shows how often the signal was above the power threshold in each time window (referred to as the number of points above threshold), and the time between each recorded signal is shown in panel (c). The maximum value for the number of points above threshold depends on the size of the time window that each signal is recorded in. If the time window is 10 μ s, the maximum is 250 and if the time window is 80 μ s, the maximum is 2000.

To accurately locate the three dimensional position of a lightning source, the LMA stations must be sufficiently separated from each other so that the signal from a source arrives at each station at significantly different times (Thomas et al., 2004). The four stations, Nikiski, K-Beach, Clam Gulch and Ninilchik, were all approximately equidistant from Redoubt Volcano due to the limitations on available station sites, with distances ranging from 77 to 81 km. In this situation, variations in the altitude of a source would not result in a large enough change in the arrival time differences between pairs of stations. For example, the difference in arrival time between the Clam Gulch and K-Beach stations will be nearly the same for a source located 5 km above Redoubt Volcano as for one 10 km above, making it impossible to determine the altitude of the source. Due to this limitation, the x (east–west) and y (north–south) positions of the sources were determined assuming a fixed altitude of 5 km. Fig. 3 shows the predicted absolute errors in the x and y locations for test data at 5 km altitude using 40 ns timing noise in the test data. The errors were determined from the covariance matrix resulting from solving the non-linear system of equations describing the arrival time of a source for the parameters x, y, and t (time) assuming a fixed z (Thomas et al., 2004). The errors in the x and y position were less than 200 m within a 50 km radius of Redoubt Volcano.

Some of the located data were processed using only the arrival times from 3 stations because there were only 3 stations operating during these particular times due to unexpected power issues. The rest of the locations were determined using arrival times from all 4 stations. This difference is noted throughout the article where pertinent.

2.2. Cloud-to-ground lightning

Locations and times of cloud-to-ground lightning were obtained from the World Wide Lightning Location Network (WWLLN)

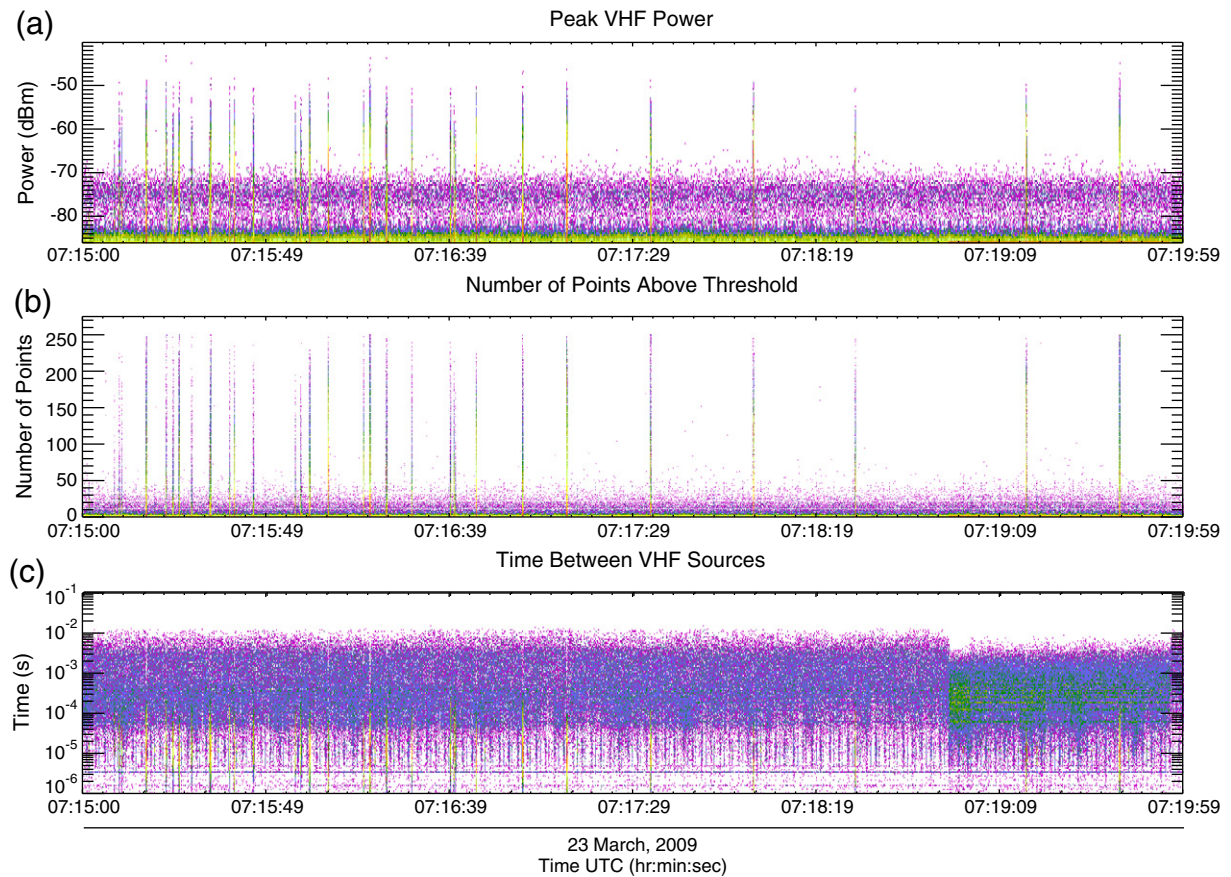


Fig. 2. Example of unprocessed (raw) lightning mapping data recorded by a single station. Panel (a) shows the peak power in units of decibel milliwatts (dBm) recorded during each 10 μ s window, panel (b) shows the number of points that were above the power threshold in each time window, and panel (c) shows the time between the recorded peaks. The apparent step and shift in colors from purple to green in panel (c) near 07:19 is due to the station's automatic adjustment in the minimum power threshold. The colors in each plot indicate the relative density of points, red being the densest and purple the least.

(Dowden et al., 2002; Rodger et al., 2005) and the Alaska BLM (T. Weatherby, pers. comm.). The WWLLN detects very low frequency (VLF) radiation from lightning and uses time of group arrival (TOGA) methods to locate the sources. Rodger et al. (2005) reported

a WWLLN detection efficiency of 26% for cloud-to-ground lightning and 10% for intracloud lightning. The Alaska BLM operates a low frequency time of arrival (TOA) lightning location network manufactured by Vaisala. The detection efficiency of this network is

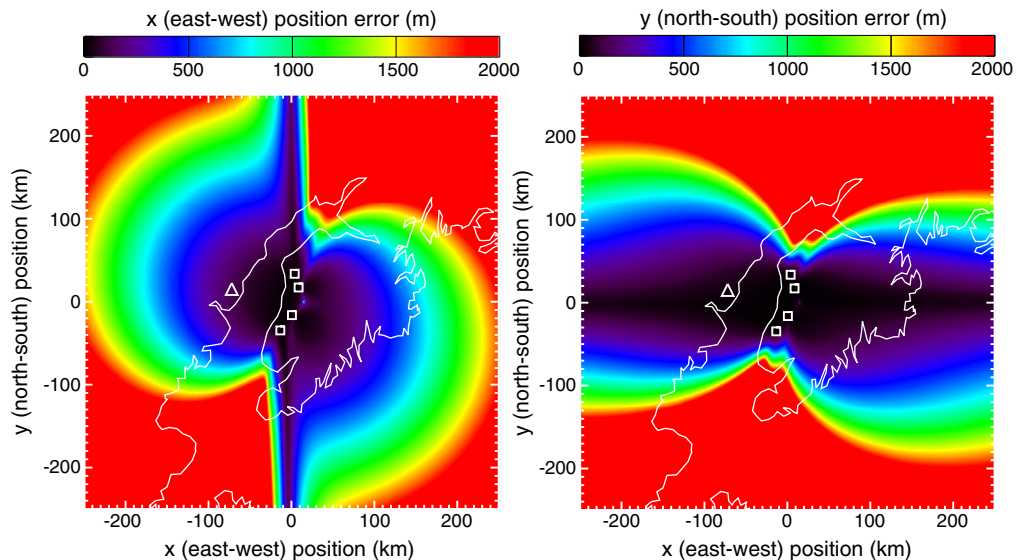


Fig. 3. Standard deviation of the x and y positions of synthetic data at a fixed altitude of 5 km. The locations of the stations are marked with white squares and the location of Redoubt Volcano is marked with a white triangle.

unknown, but is expected to be low (10–50%) because the network is optimized to detect lightning in the interior of Alaska, not in the region where Redoubt Volcano is located.

2.3. Infrasound data

This article incorporates data of infrasound waveforms, acoustic pressures and signal durations for the eruptive events. The acoustic signal is used primarily as an indicator of when and for how long an explosive event occurred. Infrasound data were obtained from a Chaparral Model 2.5 microphone installed at the DRF station approximately 12 km north–northeast of Redoubt Volcano's summit (McNutt et al., this issue). A high gain and a low gain channel were recorded during the eruption. All plots of the waveforms presented here are from the high gain channel and take into account the approximate 38 second time delay for the signals to reach the station. Signal durations (Table 1) were measured from the time when the signal amplitude increased to twice as large as the noise background to the time when the signal returned to the noise background level.

Amplitudes (peak pressure) were measured from zero to peak on the low gain channel.

2.4. Seismic data

Seismic waveforms, signal durations and reduced displacements (D_r) from the eruption were obtained from the Redoubt Volcano seismic network (McNutt et al., this issue). The instruments used were Mark Products L4-C short period (period of 1 s) seismometers. Unless otherwise noted, all of the data presented here are from the RDT station, which was approximately 21 km from the vent. All plots of the waveforms take into account a time delay of 5 s for the signals to reach the seismometer. Seismic durations were determined in a similar manner as the infrasound durations.

Reduced displacement is a calculation that provides a normalized metric for the amplitude of ground motion and has been related to ash column height (McNutt, 1994). Essentially, reduced displacement is the product of waveform amplitude and distance to the source. The calculation assumes surface wave propagation and takes instrumental magnification and geometrical spreading into account.

Table 1
Observations of lightning during the explosive events of the 2009 eruption of Redoubt Volcano.

Date (mm/ dd)	Time ^a (UTC)	Event number	Acoustic duration (min)	Acoustic pressure (Pa)	Seismic duration (min)	D_r (cm ²)	Plume height (km)	Lightning duration (min)	LMA sources (# located)	Regular flashes	Peak rate (#/min)	Small discharges	Peak rate (#/min)	Single- source discharges	Peak rate (#/min)	Cloud- to-ground discharges (BLM/ WWLLN)
03/23	06:35:54	1	26	25	–	5	5.5	2.4	558	4	1	0	0	0	0	0/0
03/23	07:02:30	2	3	151	8	13.3	14.0	20.6	48,653	573	84	527	121	5089	1664	0/5
03/23	08:14:43	3	13	38	14	8.6	14.6	29.9	116,929	1536	161	2447	276	21,792	2383	3/8
03/23	09:39:30	4	8	70	9	74	13.4	39.1	230,939	1975	170	1318	128	28,422	2519	79/172
03/23	09:48:54		12	90	30	56	13.7	n/a ^b	n/a ^b	n/a ^b	n/a ^b	n/a ^b	n/a ^b	n/a ^b	n/a ^b	n/a ^b
03/23	10:53:31		2	12	7	13	–	0	0	0	0	0	0	0	0	0/0
03/23	12:30:59	5	16	173	22	43	18.3	53.4	266,382	2739	233	4981	563	63,814	5392	11/24
03/23	12:59:32		1	14	2	45	–	n/a ^b	n/a ^b	n/a ^b	n/a ^b	n/a ^b	n/a ^b	n/a ^b	n/a ^b	n/a ^b
03/24	03:41:13	6	12	76	17	16	16.2	34.7	908,235 ^c	n/a ^d	n/a ^d	n/a ^d	n/a ^d	n/a ^d	n/a ^d	3/7
03/26	16:35:07	7	1	7	4	3	8.2	2	153	2	1	0	0	0	0	2/1
03/26	17:24:52	8	7	100	14	12	18.9	34.4	194,758	1967	175	4086	575	55,128	7186	13/1
03/27	07:47:49	9	15	31	21	12	12.5	39.9	26,550	229	35	213	55	4671	2010	18/14
03/27	08:29:00	10	4	54	9	12	14.9	38.7	165,927	1341	129	1594	252	20,714	3404	155/106
03/27	08:42:43		3	8	7	6.7	–	n/a ^b	n/a ^b	n/a ^b	n/a ^b	n/a ^b	n/a ^b	n/a ^b	n/a ^b	n/a ^b
03/27	16:12:18		0.6	4.1	0.9	1.1	–	0	0	0	0	0	0	0	0	0/0
03/27	16:39:36	11	4	83	10	22	15.5	38.6	466,833 ^c	n/a ^d	n/a ^d	n/a ^d	n/a ^d	n/a ^d	n/a ^d	41/12
03/28	01:35:21	12	2	146	9	19	14.6	30.3	70,011	534	72	501	126	5319	1535	13/3
03/28	03:24:56	13	3	138	4	8.1	15.2	34.8	116,826	930	125	1059	231	19,939	5795	53/15
03/28	07:20:17	14	2	78	2	26	12.5	41.1	62,174	462	74	537	138	6326	1449	14/32
03/28	09:20:02	15	2	59	2	3.6	14.6	42.8	54,476	445	65	430	110	5130	1367	28/39
03/28	10:00:15		<1	10	6	13	–	0	0	0	0	0	0	0	0	0/0
03/28	16:11:19		0.5	2	0.5	1.2	–	0	0	0	0	0	0	0	0	0/0
03/28	21:40:38	16	2	28	12	5.7	5.2	0	0	0	0	0	0	0	0	0/0
03/28	23:09:37		3	5.9	1	2.3	–	0	0	0	0	0	0	0	0	0/0
03/28	23:30:03	17	3	67	37	30	12.5	40	90,145	1013	142	900	173	8246	1830	12/0
03/29	03:24:09	18	4	49	44	5.2	14.6	23.2	63,234	629	98	577	108	5600	1504	6/7
03/29	19:19:45		–	–	2	6.8	6.1	7.9	1214	8	2	0	0	0	0	0/0
03/30	07:11:33		–	–	3	4.3	6.1	4.4	1149	9	4	0	0	0	0	0/0
03/30	17:43:46		–	–	4	7	–	0	0	0	0	0	0	0	0	0/0
03/30	18:50:36		–	–	5	0.6	6.1	<1	18	1	1	0	0	0	0	0/0
03/31	07:31:28		6	1.3	7	3.8	6.1	6.2	524	6	2	0	0	0	0	0/1
03/31	07:41:54		0.3	0.25	0.5	2.4	–	n/a ^e	n/a ^e	n/a ^e	n/a ^e	n/a ^e	n/a ^e	n/a ^e	n/a ^e	0/0
04/01	00:07:00		<1	1.9	10	1.7	4.6	3.8	921	5	2	0	0	0	0	0/0
04/01	03:46:29		0.5	0.4	0.5	3.5	–	0	0	0	0	0	0	0	0	0/0
04/04	13:57:43	19	19	38	19	10.7	15.2	69.8	618,009	6841	316	10,376	497	130,635	6548	40/30
04/04	14:16:26		12	88	56	15.3	15.2	n/a ^b	n/a ^b	n/a ^b	n/a ^b	n/a ^b	n/a ^b	n/a ^b	n/a ^b	n/a ^b
04/05	18:36:51		1	3.7	1.5	7.7	–	0	0	0	0	0	0	0	0	0/0

^a Time of explosive event is the arrival time at the DRF station. There was an approximate travel time of 38 s between the vent of the volcano and the station.

^b A volcanic lightning storm was already occurring due to the previous event when this explosive eruption occurred. All lightning statistics are included in the entry for the previous event.

^c LMA source locations were determined using 3 station data because only 3 stations were operating at the time. The total number of located LMA sources are not comparable to events processed with 4 station data.

^d Statistics on numbers and rates of discharges were excluded because the locations were determined with 3 station data.

^e A weak electrical event was already occurring due to the previous event when this explosive eruption occurred. All lightning statistics are included in the entry for the previous event.

2.5. Eruption column heights and radar

Radar observations of the plumes during the eruption were obtained from the FAA NEXRAD radar in Anchorage, AK and the USGS-operated EEC Minimax 250C Doppler radar in Kenai, AK. The USGS radar operates in C-band at 250 W (Schneider and Hoblitt, [this issue](#)). Peak column heights for each eruptive event were determined by comparing observations from NEXRAD and the USGS radar and selecting the observation that gave the higher altitude. Each column height measurement corresponds to the center of the beam. Because the radar beam must be at least 50% full to give a return, each measurement represents the minimum peak altitude of the column. The uncertainty in the column height measurements are +1.3 km (for NEXRAD) and +2.3 km (for USGS). The USGS radar was also used to determine the column height soon after the onset of the explosive eruption on 28 March at 0324 UTC.

2.6. Data from the 2006 eruption of Augustine Volcano

The Redoubt Volcano lightning observations are compared to the previous observations of lightning from the 2006 eruption of Augustine Volcano, located in south-central Alaska. The LMA data from the Augustine Volcano eruption presented here is from the two-station array that was located on the Kenai Peninsula in late January 2006 (Thomas et al., 2010). The LMA was operating in 80 μ s mode during this deployment. Infrasound data are from the AUE station on Augustine Volcano and seismic data are from the Oil Point station (OPT) (McNutt et al., 2010).

3. Results and discussion

Here we present our observations of lightning during the eruption of Redoubt Volcano. We first present typical examples of the electrical activity that occurred during distinct explosive events and compare it to the electrical activity observed during previous studies of Augustine Volcano. We then show how the lightning during an explosive event evolved and what that implies for the charge structure of the

plume. The physical types of discharges are then described according to classifications previously defined by (Thomas et al., 2010). Finally, the overall amount of electrical activity from each event is compared to several parameters of the eruptive activity, which has implications for the electrification processes of the plume.

3.1. Typical examples of electrical activity

We observed 23 distinct episodes of electrical activity associated with explosive activity, as described in Table 1. During larger explosive events, like event 2 on 23 March at 07:02 UTC, we observed what we describe as a volcanic lightning storm. These storms had durations between 20 and 70 min and commonly had more than 1000 lightning flashes. Sixteen distinct volcanic lightning storms were observed during the 2009 eruption. During smaller events, such as the event on 1 April at 00:07 UTC, we saw either no lightning or just a few lightning discharges over spans of less than 10 min. We refer to the events that had only a few discharges as weak electrical events. Weak electrical events were observed subsequent to 7 of the smaller explosive events. In the following sections we present typical examples of a volcanic lightning storm and a weak electrical event and compare both types of electrical activity to previous observations of volcanic lightning from the 2006 eruption of Augustine Volcano.

This article uses many terms to describe the phases of eruptive and electrical activity and the types of discharges that occurred, as summarized in Fig. 4. The temporal sequence of the phases is shown along with the temporal variation of the typical rates of the various categories of electrical activity. Black and white gradient bars illustrate the frequency of each type of discharge, black being most frequent and white being least frequent. The electrical activity is categorized in two different groups. The first group describes the three physical types of discharges observed and the second describes the three classifications of discharges used by the flash algorithm (see Appendix A). The flash algorithm classified discharges based on the number of lightning sources in each discharge; this classification is

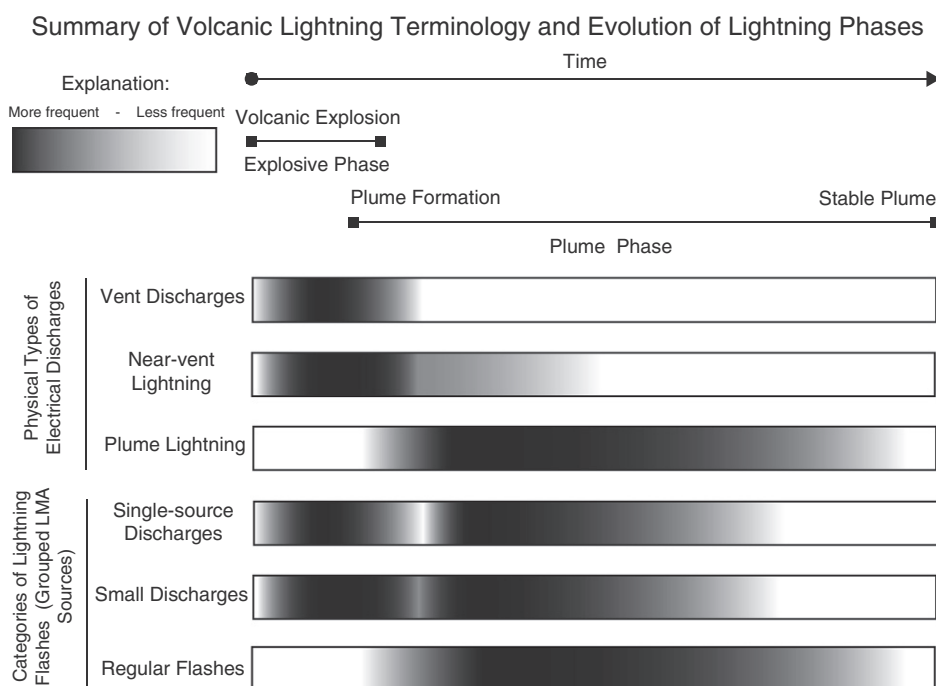


Fig. 4. Summary of the terminology used to describe phases of volcanic and electrical activity, the physical types of lightning discharges observed during explosive volcanic eruptions, and categories of lightning flashes as grouped using a flash algorithm. The black and white gradient bars indicate when each type of discharge was typically observed, black being most frequent and white least frequent. The phrase 'stable plume' refers to a fully developed plume that is no longer convectively active.

used in conjunction with other information to determine the physical type of each discharge, which is discussed further in Section 3.4.

3.1.1. Volcanic lightning storm on 23 March 2009 at 07:02 UTC

The first large explosive event of the eruption occurred on 23 March at 07:02 UTC and produced a typical volcanic lightning storm. Compared to the rest of the explosive eruptions, this was a relatively short duration event, but was strong enough for the plume to reach 14 km. Seismic and acoustic signal durations were 8 and 3 min (Table 1), respectively. The amount of lightning produced in the

plume was also low compared to other events. The volcanic lightning storm had a duration of 20.6 min and produced a total of 48,653 located LMA sources, which translated to 573 regular flashes and 527 small discharges. A comparison of the electrical, seismic and acoustic activity is shown in Fig. 5. The volcanic lightning storm propagated north–north-east of the volcano, presumably due to the wind blowing the plume in that direction, with the farthest sources located about 28 km from the vent, as shown in Fig. 6. The colors of the sources in Fig. 6 indicate the progression of time, blue being earliest and red latest, which demonstrate that the lightning activity towards the end of the storm (yellow

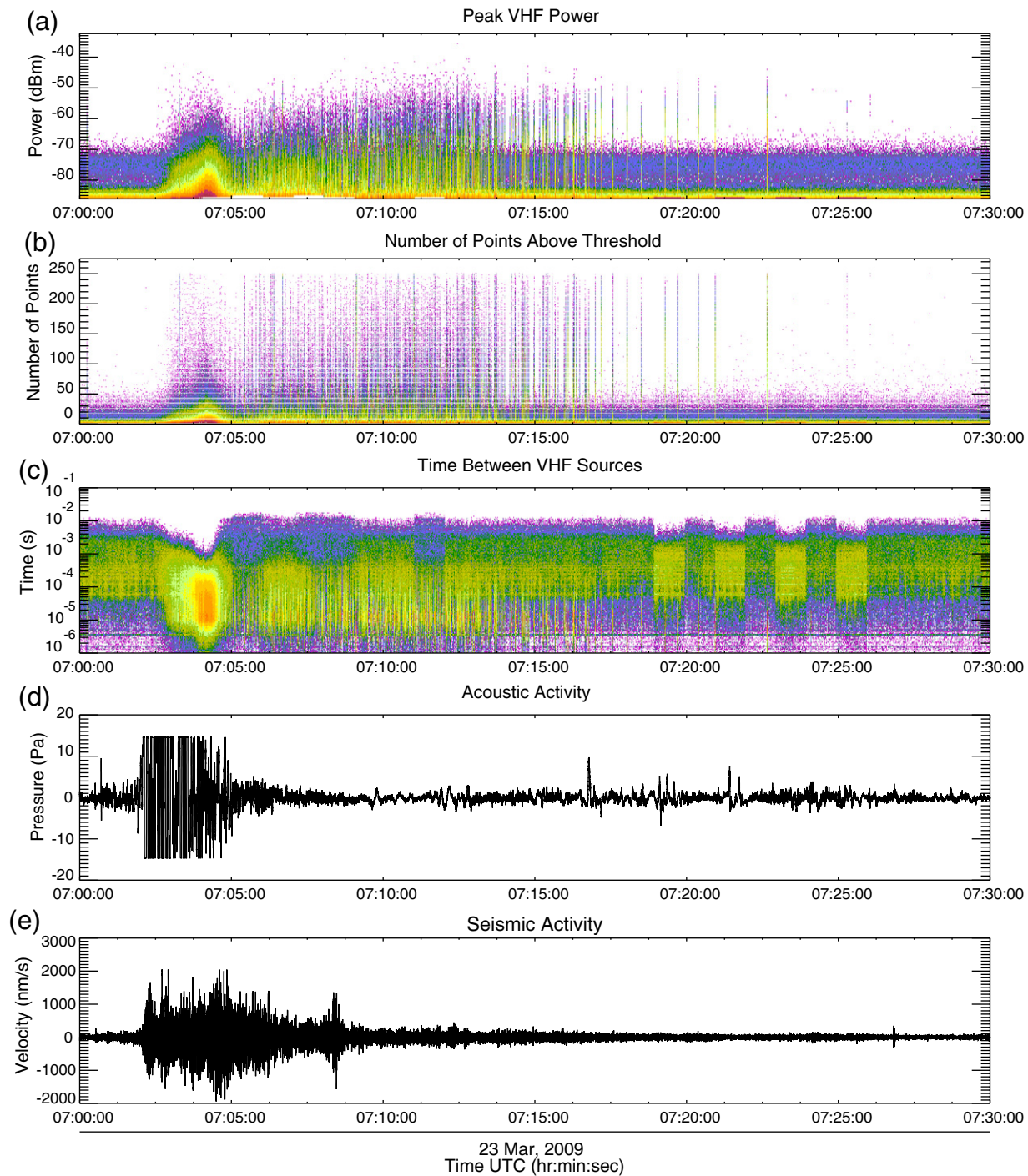


Fig. 5. Unprocessed (raw) LMA, acoustic and seismic data from explosive event 2, 23 March at 07:02 UTC. Panels (a), (b), and (c) show the peak received power, number of points above threshold and the time between recorded peaks from the Clam Gulch LMA station. The steps and shifts in coloring visible between 07:19 and 07:26 in panel (c) are caused by changes in the minimum power threshold. The colors indicate the relative density of sources, red being the densest and purple the least. Panels (d) and (e) show the acoustic signal from the DFR station and the seismic signal from the RDT station. Both signals have been time-shifted to account for the travel time delay.

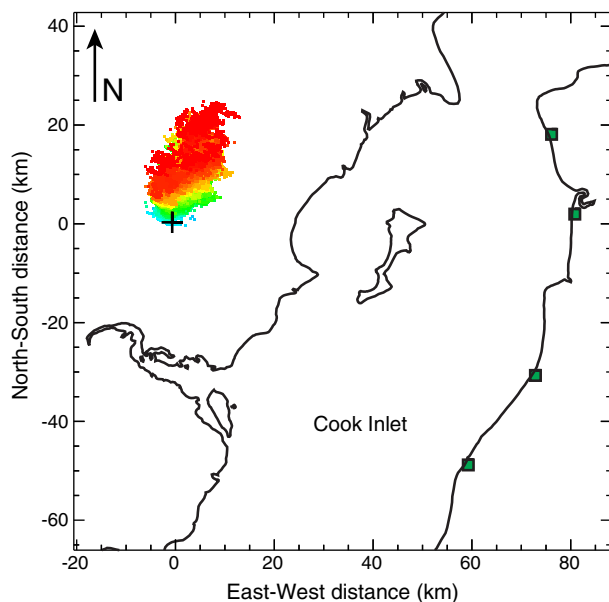


Fig. 6. Located LMA data from the 23 March 07:02 UTC event (explosive event 2), shown in plan position. The colors indicate the progression of time, blue being earlier times and red later times. The activity at the beginning of the volcanic lightning storm (blue and green sources) is mostly covered up by the later activity (red sources), and covers a larger area than what is visible in the figure. Redoubt Volcano is located at the coordinates (0,0) (black cross), station locations are marked with green squares.

and red sources) was not anchored to the vent and the storm as a whole had moved off the vent.

There are two distinct features in the peak received power shown in panel (a) of Fig. 5: the strong and continuous signal at the beginning, and the discrete electrical signals that followed. To illustrate the differences of these two features, four 30-second segments of time were selected from the peak power for comparison. The 4 segments of the peak power are shown on expanded scales in Fig. 7. Segment 1 is from the initial period of strong continuous activity, segments 2 and 3 are from periods of high rate discrete activity, and segment 4 is from a period of low rate discrete activity at the end of the storm. The signal from segment 1 is clearly more continuous than segments 2–4, which have obvious spikes in activity separated by periods of less activity. To further demonstrate these differences we examined the rate of recorded sources for each of the four segments. In order to fairly compare the source rates from the 4 segments to Augustine Volcano, the Redoubt Volcano data were decimated from 10 μ s mode (maximum of one recorded source per 10 μ s) to 80 μ s mode (maximum of one recorded source per 80 μ s), which was used during the Augustine Volcano experiment. The peak power data for both Redoubt Volcano and Augustine Volcano were then normalized to be the power at a distance of 100 km from each volcano (the VHF data shown in Figs. 7 and 9 do not have this normalization applied, however.). An artificial power threshold was then applied to the data to eliminate most of the local noise. Only sources with a power greater than or equal to -78 dBm were included in the source rate plots and average rate calculation. Fig. 8 shows the number of recorded sources in successive 10 ms intervals during the time period of each segment. The average number of sources per 10 ms over each 30 second time period for segments 1 through 4 were 8.5 (std dev 7.4), 3.7 (std dev 11.0), 3.9 (std dev 12.0), and 2.0 (std dev 10.4), respectively. In the 80 μ s mode the maximum number of sources in 10 ms is 125. As shown in Fig. 8, the source rate for segment 1 did not vary greatly over time compared to the rates for segments 2, 3 and 4, which had spikes in the source rate associated with discrete lightning flashes. This is also reflected in the standard deviation

of the average calculation for each segment. The signal from segment 1 is referred to as a ‘continual RF’ signal due to the relatively high and steady average source rate (this is not meant to imply that the electrical activity that produced this signal was radiating continuously), and the spiky nature of the source rate for segments 2, 3, and 4 leads us to call these types of signals ‘discrete electrical activity.’

It is also important to point out that the continual RF signal in this example began while the volcano was actively erupting and producing ash, as determined from the infrasound observations. The continual RF signal tapered off and ended at the same time that the acoustic signal began to return back to the background level. Similarly, in all other storms the continual RF signal was also observed during the actual eruptive event.

3.1.2. Comparison of the volcanic storm with the 2006 eruption of Augustine Volcano

Previous observations of lightning from a relatively large explosive event during the 2006 eruption of Augustine Volcano, shown in Fig. 9, revealed that electrical activity occurred in two separate phases: the explosive phase and the plume phase (Thomas et al., 2007; Thomas et al., 2010). The initial continual RF signal was referred to as the explosive phase because it occurred concurrently with the explosive eruption. The discharges that gave rise to this signal were inferred to have occurred directly above Augustine Volcano at low altitude. This is because the explosive phase discharges were only observed by the station that had a direct line-of-sight view to the vent (the other station was situated inland and could not see the volcano but could see above it). The set of discrete discharges that occurred subsequent to the continual RF signal was referred to as the plume phase because the discharges occurred progressively over and downwind of the volcano in the drifting plume.

The explosive and plume phases observed at Augustine Volcano were also observed during the volcanic lightning storms at Redoubt Volcano, which allowed us to make a more concrete description of the two phases. The continual RF signal shown in Fig. 7b, characterized by the relatively high average source rate with lower variability (8.5 [std dev 7.4] sources per 10 ms) is a typical example of an explosive phase signal. The discrete activity shown in Fig. 7c–e, characterized by a lower average source rate but with higher variability (averages between 2.0 [std dev 10.4] and 3.9 [std dev 12.0] sources per 10 ms) are typical examples of a plume phase signal. Similar patterns in the source rates for continual and discrete activity were also observed during the eruption of Augustine Volcano, shown in Fig. 10. During continual RF activity at Augustine Volcano (05:31:25 to 05:31:55 UTC on 28 January, 2006), the average number of sources per 10 ms was 34.8 (std dev 9.0), significantly larger than what was observed at Redoubt Volcano. The average number of sources per 10 ms during low rate (05:42:10 to 05:42:40) discrete activity at Augustine Volcano was 3.3 (std dev 17.8), similar to what was observed at Redoubt Volcano (there was no corresponding time of high rate discrete activity at Augustine Volcano). The key difference between continual and discrete signals is the standard deviation, which shows the variability in the source rate. The continual RF is characterized by source rates that do not vary over relatively long time periods (30 s, for example), while the discrete signals are characterized by high variability in the source rates over relatively long time periods. In the rest of this article the explosive and plume phase terminology will be used to describe the time periods when the peak VHF rates met similar standards.

The Augustine Volcano results showed that the two phases of electrical activity were caused by separate electrification mechanisms (Thomas et al., 2007; Thomas et al., 2010). The explosive phase discharges occurred concurrently with the explosive eruption, therefore it is believed that these discharges came about because the ejecta from the volcano was charged during the eruption process. Charge generation by the fracturing of magma, known as fractoemission

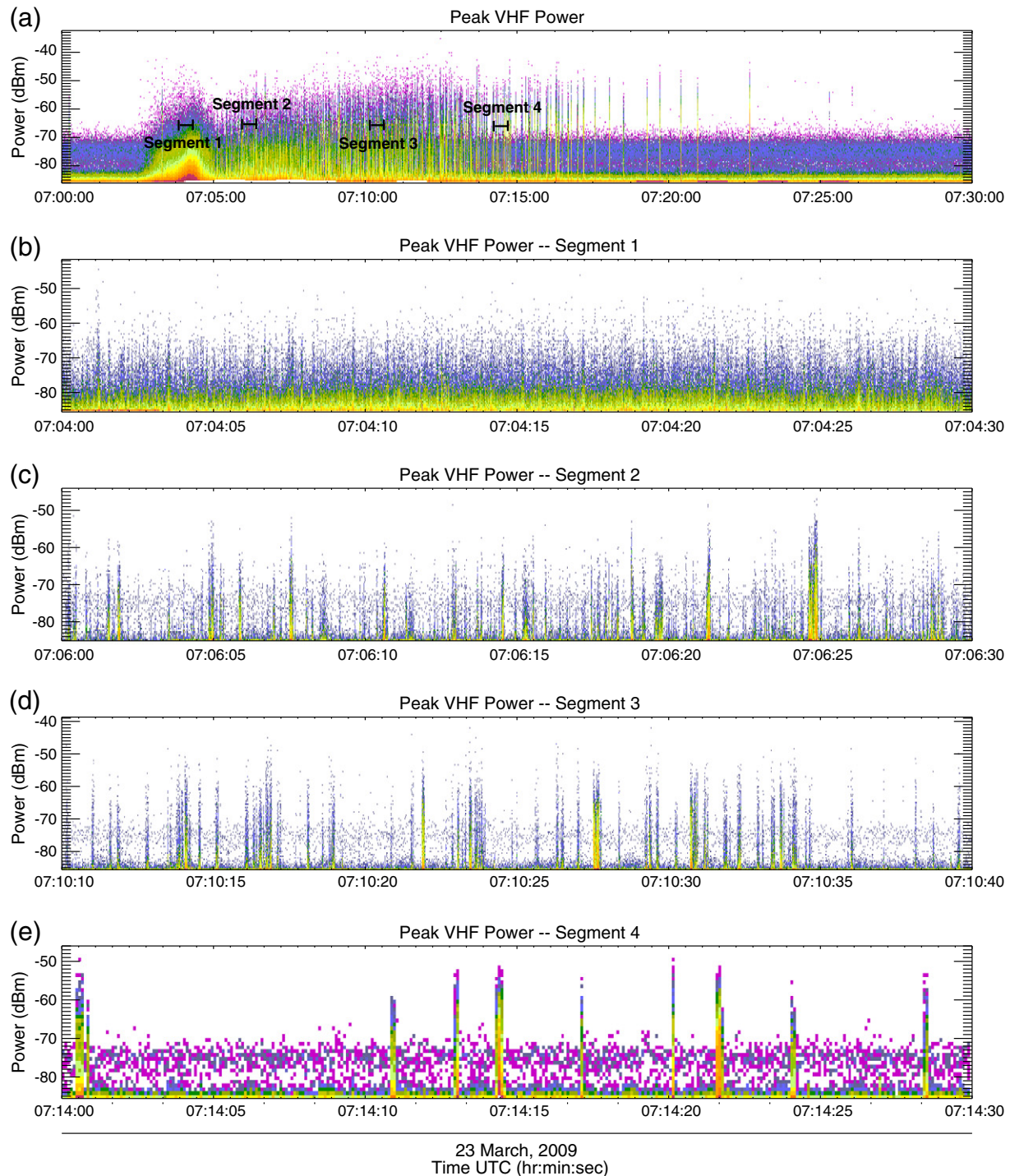


Fig. 7. Selected segments of time of the peak VHF power from the 23 March 07:02 event plotted on expanded time scales. Each segment is 30 s in duration. The size of the points in each panel is relative and has no significance.

(James et al., 2000), is thought to be the dominant charge mechanism for silica-rich plumes (James et al., 2008), though boiling of surface water (such as ice or snow) may contribute to electrification as well (James et al., 2008). In addition to charge generation through rapid boiling, ice and snow covering the volcano could potentially increase the electrification by adding a phreatomagmatic component, which would create a finer grained ash and therefore provide more charge carriers. As for the plume phase lightning, the period of inactivity between the explosive and plume phases suggests that electrification

processes in the plume were taking place in order to give rise to the plume lightning. These processes could simply involve the gravitational separation of the already-charged ash or could be a result of water-based charging mechanisms that are responsible for thunderstorm lightning (e.g., Williams, 1985). Water-based charging mechanisms rely on collisions between differing types of ice particles (e.g., graupel and ice crystals), therefore ambient atmospheric conditions play a role in water charging mechanisms (plumes must be cold enough to create ice). Further discussion on plume charging

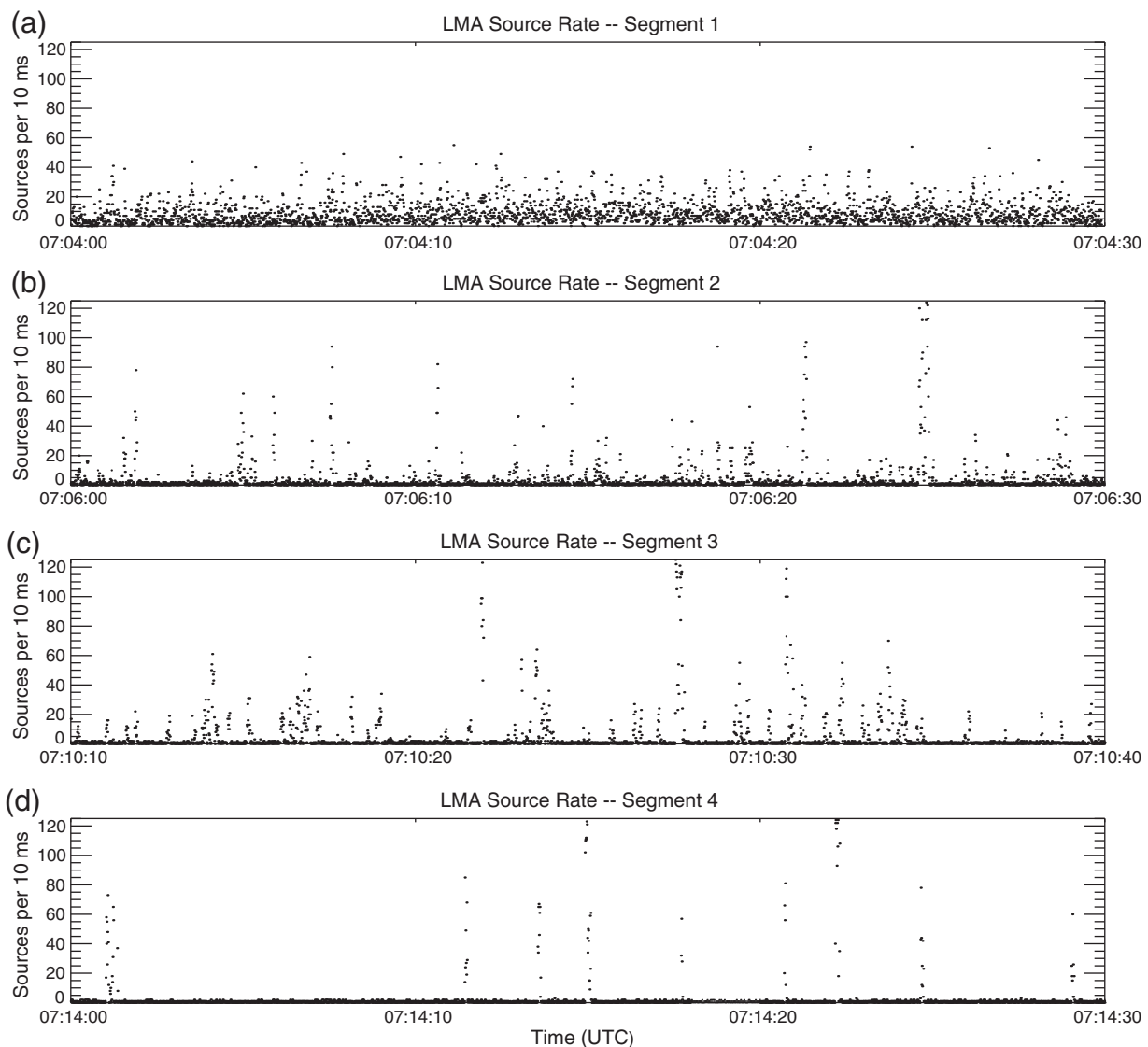


Fig. 8. Number of LMA sources per 10 ms for each of the 4 power segments shown in Fig. 7.

mechanisms during the Redoubt Volcano eruption will be presented in Section 3.5.

Though the explosive and plume phases occurred at both Redoubt Volcano and Augustine Volcano, there were differences in these phases among the two eruptions. First, we had predicted that the explosive phase signal at Redoubt Volcano would be as strong or stronger than Augustine Volcano because the eruption was bigger and more energetic, however the average source rates observed during the explosive phase at Redoubt Volcano were lower than Augustine Volcano. Redoubt Volcano differs from Augustine Volcano in that it had more snow and ice cover (Trabant and Hawkins, 1997), but we would expect this to increase electrification, not decrease it. This suggests that much of the continual RF activity was being blocked from view at the stations by the eastern ridge, and that the intensity of this activity decreased quickly with altitude. Secondly, the plume phase signal from the Redoubt Volcano observations often overlapped with the explosive phase signal, unlike Augustine Volcano, where a lull of several minutes was observed between the two phases. The electrical activity at Redoubt Volcano was even so intense at times that the two phases were difficult to distinguish from each other. We assume this is also because the Redoubt Volcano eruption was overall more energetic than the Augustine Volcano eruption. We expect a more energetic eruption to produce more plume phase

lightning regardless of the charging mechanism, since a more energetic eruption would produce both more ash and larger column heights, which would influence both ash and water-based charging mechanisms. Furthermore, the atmospheric conditions during the Redoubt Volcano and Augustine Volcano eruptions were similar, and probably did not affect electrification. Finally, the explosive phase lightning at Augustine Volcano started concurrently with the explosive event, while at Redoubt Volcano there were delays ranging from 30 to 40 s to several minutes between the eruption onset and the beginning of the explosive phase.

The reason for the observed delay between the start of the eruption and the start of the explosive phase lightning at Redoubt Volcano is not clear, but it is very likely that the eastern ridge on Redoubt Volcano is responsible for the delay. The delay between the start of the eruption and the start of the explosive phase lightning at Redoubt Volcano was mostly likely caused by the electrical activity being blocked by Redoubt Volcano's eastern ridge. Due to the difference in the source rates of the continual RF activity between Redoubt Volcano and Augustine Volcano, we are fairly certain that there was electrical activity occurring behind the ridge that the stations couldn't see. But because of the eastern ridge on Redoubt Volcano, we do not know when the electrical activity actually began. If we assume that the electrical activity began right at the onset of the eruption as was observed

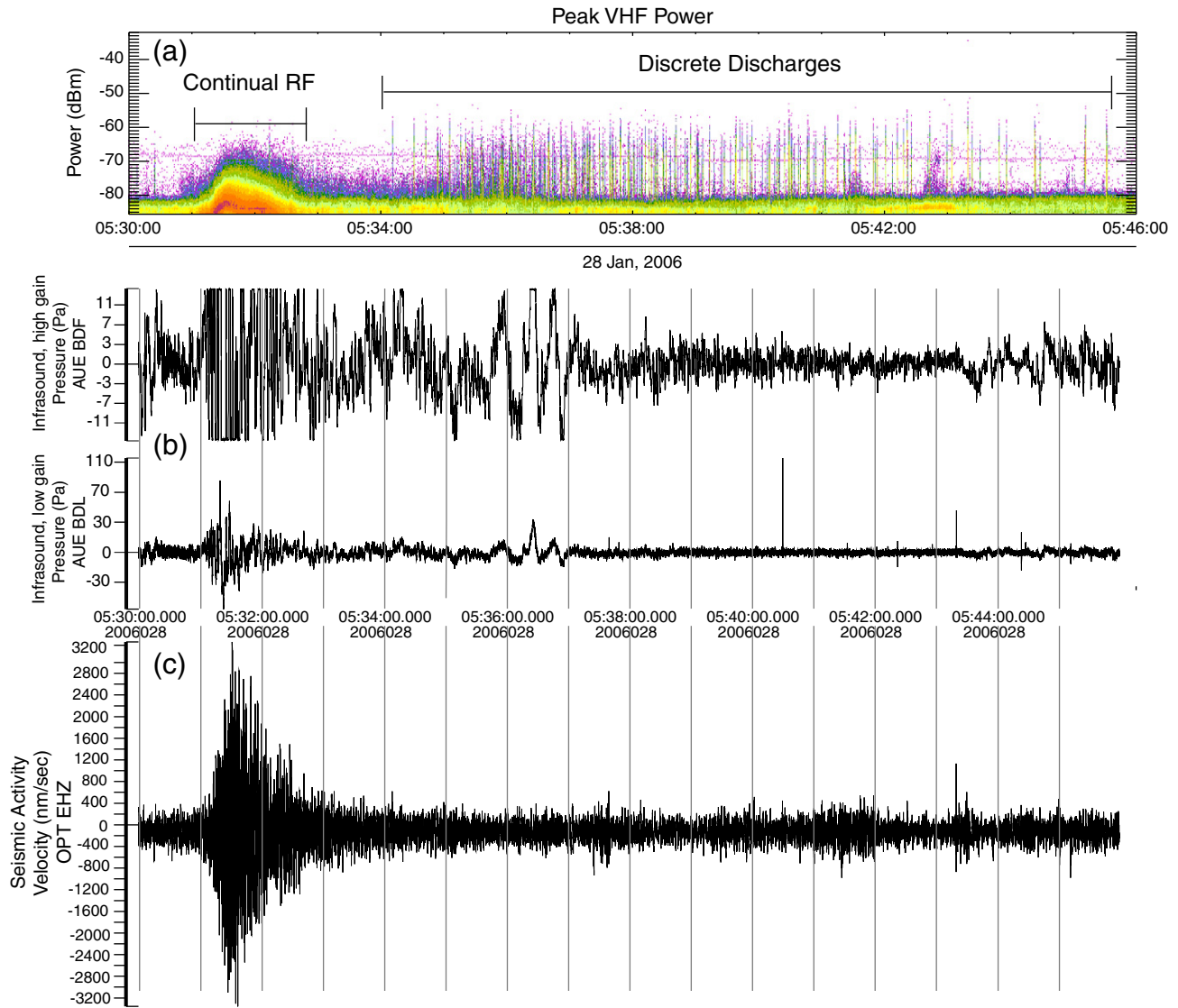


Fig. 9. Unprocessed (raw) LMA, acoustic and seismic data from the explosive eruption on 28 January 2006 05:31 UTC of Augustine Volcano. Panel (a) shows the peak VHF power received by the station located in Homer. Panels (b) and (c) show the acoustic signal from the AUE station and seismic signal from the OPT station. Both signals have been time-shifted to account for the travel time delay.

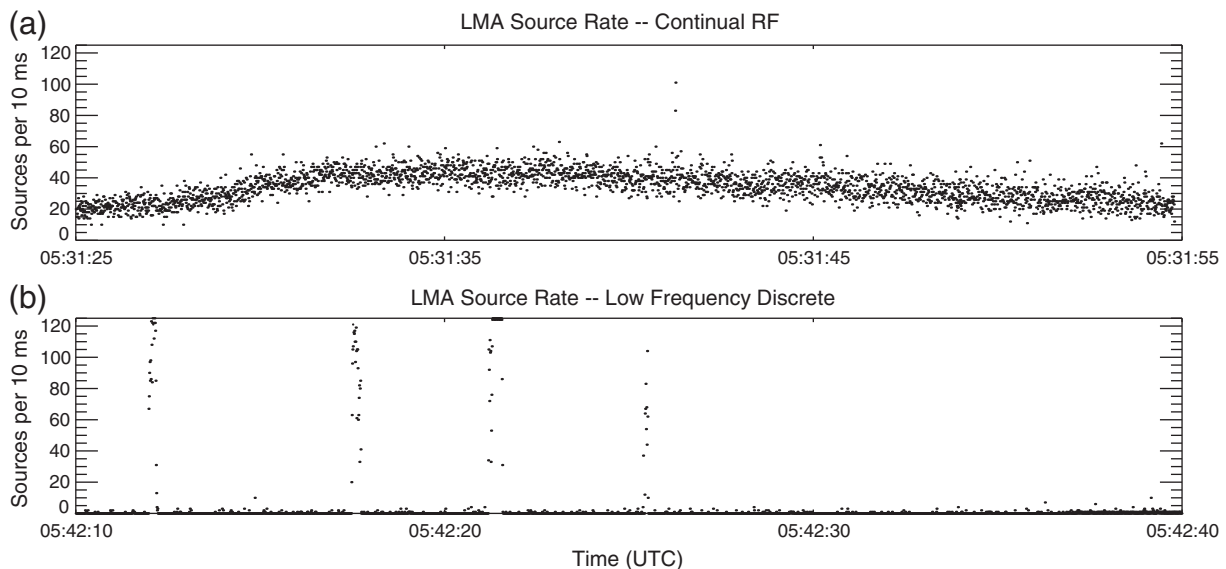


Fig. 10. Number of LMA sources per 10 ms for 30 second periods of continual RF and low rate discrete electrical activity during the eruption of Augustine Volcano.

for Augustine Volcano, then we would expect the electrical activity to have begun at low altitude and be initially blocked from the view of the stations by the ridge. And because we do see this electrical activity above the ridge, one might also assume that any electrical activity occurring behind the ridge would simply extend above it once the eruption column was higher than the ridge. At a speed of 100 m/s, it would take about 6 s for volcanic material to get above the ridge, and a few more for it to get in the line of site of the stations. However, the observed time delays were significantly longer than 6 s, and the events with large amounts of lightning tended to have delays between 1 and 3 min. The long delay implies that the electrical activity was initially confined to low altitudes right above the vent and didn't increase in altitude linearly with time as assumed above. The vertical extent of the continual RF activity is probably related to the intensity (mass eruption rate) of the eruption, so as the intensity increases, the extent of the region where these discharges are produced also increases. As demonstrated in Fig. 5 the intensity (rate of recorded sources, indicated by the colors) of the continual RF signal between 07:02:30 and 07:05:30 similarly increased to a peak over time and then decreased. If the delay between the onset of the eruption and the onset of explosive-phase lightning was real there is unfortunately no indication that differences in the eruptive conditions between Redoubt Volcano and Augustine Volcano were responsible for it.

3.1.3. Weak electrical event on 1 April 2009 at 00:07 UTC

An example of a weak electrical event following the small explosive eruption on 1 April at 00:07 UTC is shown in Fig. 11. Electrical activity began approximately 9 min after the start of the eruptive event. The continual RF signal described in the previous example was not observed during this event, nor was the intense swarm of discrete

lightning discharges. The observed lightning consisted of five discharges over a period of 3.8 min following the small explosive eruption. The discharges were generally located over Redoubt Volcano, as shown in Fig. 12. The electrical activity observed during the other weak electrical events was very similar to this example. In other weak electrical events, such as the event on 29 March at 19:19 UTC, the lightning discharges were observed both over and to the north of Redoubt Volcano, up to 12 km away.

3.1.4. Comparison of the weak electrical event with the 2006 eruption of Augustine Volcano

During the eruption of Augustine Volcano, Thomas et al. (2010) made similar observations of small amounts of lightning following relatively small explosive events. Continual RF signals and small amounts of discrete discharges were observed during these small events. The discrete discharges were located at Augustine Volcano, not downwind of the volcano, and therefore were part of the explosive phase activity and thus caused by explosion-based charging mechanisms. There was not any direct evidence that subsequent electrification processes occurred in the small plumes because plume lightning was not observed during the smaller explosive events at Augustine Volcano.

The electrical activity observed during the 1 April weak electrical event is most likely entirely explosive phase activity, similar to what was observed at Augustine Volcano, though plume phase activity was observed during other weak electrical events. Even though continual RF signals were not observed, the discrete discharges observed during the 1 April weak electrical event were located above Redoubt Volcano, and were thus likely explosive phase activity. The eastern ridge on Redoubt Volcano may have prevented observation of the continual RF

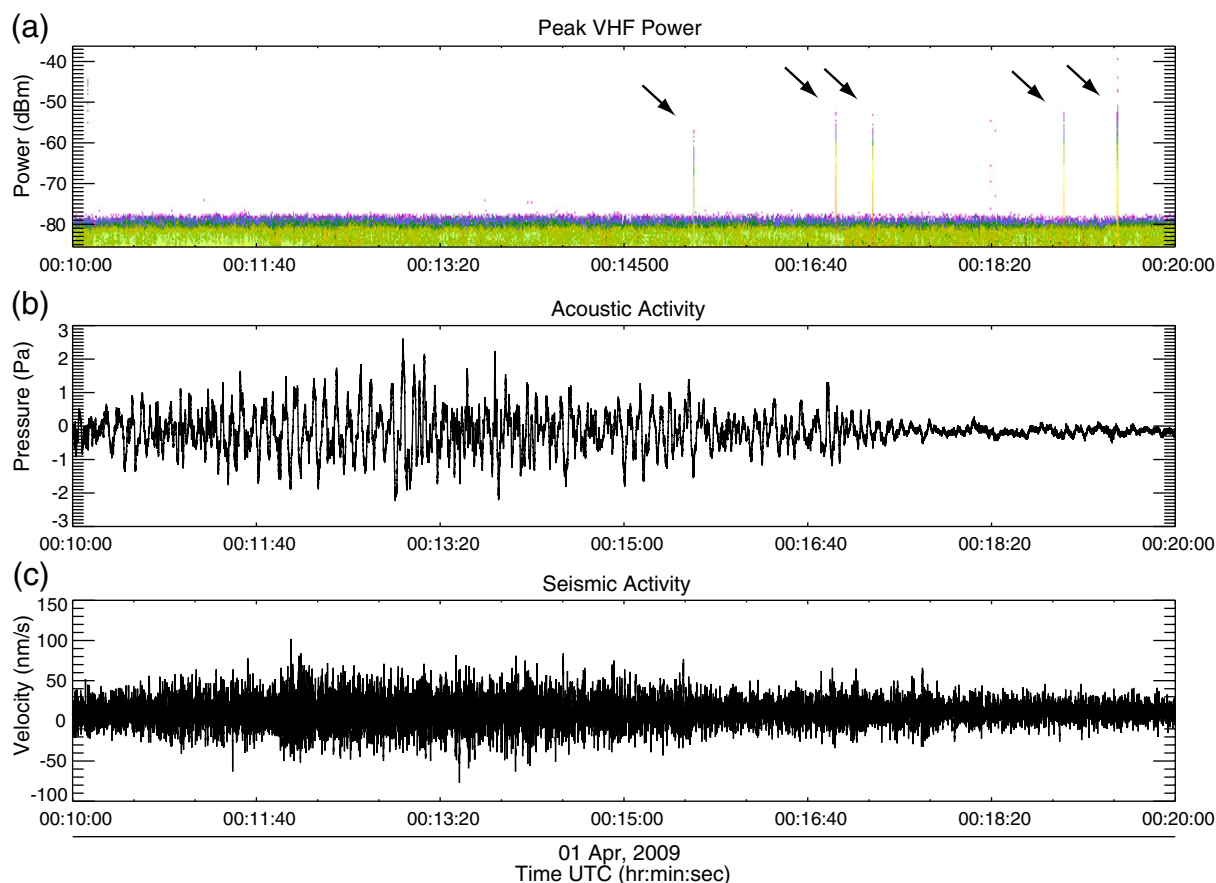


Fig. 11. Unprocessed (raw) LMA, acoustic and seismic data from the 1 April 00:07 UTC explosive event. Panel (a) shows the peak received power from the Clam Gulch station. The colors indicate the relative density of sources, red being the densest and purple the least. Arrows in panel (a) point to the discharges. Panels (b) and (c) show the acoustic signal from the DFR station and the seismic signal from the RDT station. Both signals have been time-shifted to account for the travel time delay.

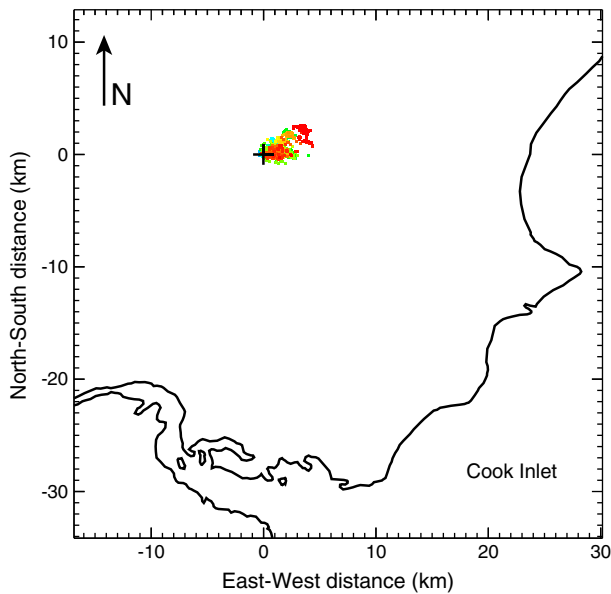


Fig. 12. Located LMA data from the 1 April 00:07 event, shown in plan position. The colors indicate the progression of time, blue being earlier times and red later times. Redoubt Volcano is located at the coordinates (0,0) (black cross).

signal, but it is also possible that no continual RF activity occurred. The source altitudes would make it easier to determine if any of the discharges were confined to the plume and thus qualified as plume phase lightning. However, discrete discharges observed during several of the other weak electrical events, (e.g., 29 March 19:19 UTC) did occur away from Redoubt Volcano (up to 12 km away) and are considered to be plume phase discharges caused by electrification mechanisms in the plume.

3.2. Evolution of lightning discharges during volcanic lightning storms

Each lightning signal recorded by the LMA is from the formation or extension of a lightning channel, and hundreds of thousands of signals may be recorded during a single storm. Each lightning flash is made up of a group of physically joined channels, extending out from an initiation site and branching in different directions. The located signals, often referred to in this article as sources or located LMA sources, outline the flash, showing its size and extent. Each source represents a piece of a discharge that is on the order of 100 m in length, but may vary from a few tens of meters to several hundred meters. From the individual measurements there is no way of knowing how many flashes there were or which sources corresponded to which flash. By looking at the source locations in time it is often easy to see the groups of sources that make up a flash. To automate this, a flash algorithm was used to sort the located sources that were close in time and space into individual flashes, which allowed us to study flash characteristics in a storm (e.g., flash area and flash rate). The algorithm used on this data set is a modification of a previously existing algorithm and is described in Appendix A. The previous algorithm worked well on most meteorological thunderstorms, but did not perform well on the Redoubt Volcano lightning because of the high data rate and unique features of volcanic lightning.

The located lightning signals recorded during Redoubt Volcano's volcanic lightning storms were grouped into three categories of discharges: regular flashes (groups of 10 or more sources), small discharges (groups of less than 10 sources) and single-source discharges. These categories only describe the number of sources in the discharges. Section 3.4 describes the physical types of the discharges, which are determined by combining the number of sources

with when and where in the plume the discharges occurred. In this section we present examples of how the rates of each discharge category and the sizes of the discharges change over time.

3.2.1. Rates and sizes of lightning flashes

The electrical activity during the explosive phase of a volcanic lightning storm was dominated by single-source discharges and small discharges, while plume phase activity was marked by an increase in the rate of regular flashes. Fig. 13 demonstrates how the rate of total located LMA sources, regular flashes, small discharges, and single-source discharges varied over the lifetime of the storm resulting from the explosive eruption on 23 March at 07:02 UTC. The explosive eruption began at approximately 07:01:52 (this is the estimated origin time, determined by subtracting the approximate travel time from the arrival times in Table 1) and stopped around 07:05:00, according to the infrasound data. Explosive phase electrical activity began at 07:02:50, about 1 min after the onset of the explosion. The explosive phase activity consisted of mostly small discharges and single-source discharges. Explosive phase activity peaked between 07:04 and 07:05 with rates of approximately 120

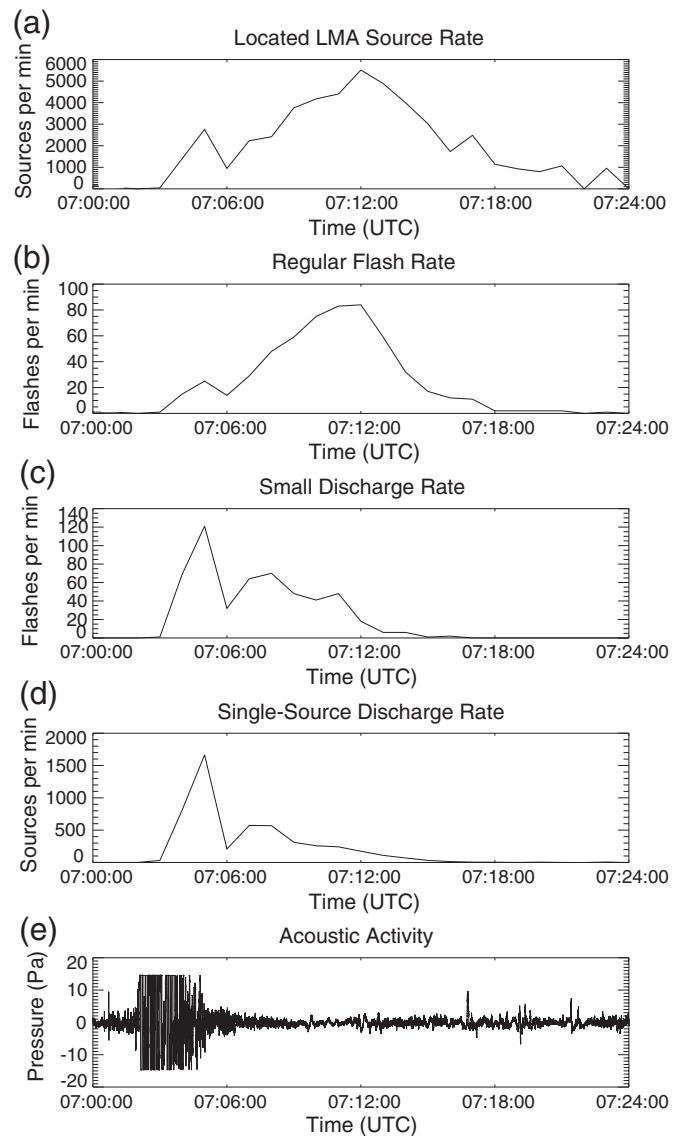


Fig. 13. The rate of total located LMA sources (panel a), regular flashes (panel b), small discharges (panel c), and single-source discharges (panel d), and the acoustic activity (panel e) during the volcanic lightning storm on 23 March at 07:02 UTC. The acoustic signal has been time-shifted to account for the travel time delay.

small discharges and 1700 single-source discharges per minute. During this peak the rate of regular flashes was only 25 per minute. After a brief decrease in activity, the rate of regular flashes increased as the electrical activity transitioned to plume phase activity. The peak rate of regular flashes was approximately 85 per minute. Significant amounts of small discharges and single-source discharges were also observed during the plume phase, though they did not dominate the electrical activity as much as they did in the explosive phase.

By comparing Figs. 8 and 13, it can be seen that only a small fraction of the signals recorded at Clam Gulch, our most sensitive station, were located during the peak of explosive phase activity. The average number of recorded sources per 10 ms during the continual activity shown in Fig. 8 was 8.5, which corresponds to an average of 51,000 sources/min. The actual per-minute rate of recorded sources during this particular time period is on the order of 3.0×10^5 sources/min, much greater than what is shown in Fig. 8 because the data in that figure were decimated and artificially thresholded (reducing the source rate) in order to be comparable to the Augustine Volcano data. Compared to the peak of 1700 sources/min shown in Fig. 13, this shows that roughly 0.5% of the signals were located. The number of located sources is limited by the least sensitive station, which in this case was about 10 dB less sensitive during this volcanic lightning storm.

Fig. 14 shows the variation of the rates of electrical activity during the 29 March 03:24 storm, which had less explosive phase activity than the 23 March 07:02 storm. According to infrasound data, the explosive eruption began at approximately 03:23:31 and ended around 03:27:31. Explosive phase electrical activity began at 03:25:10, about 1.5 min after the onset of the explosion. Between 03:26 and 03:27, explosive phase lightning was at its peak, with rates of approximately 400 single-source discharges/min, 40 small discharges/min, and 10 regular flashes/min. The total number of located sources (and the total number of recorded sources) during the explosive phase of this storm was much less than the explosive phase of the 23 March 07:02 storm, which demonstrates how the strength (peak source rate and duration of sources) of the explosive phase varied between explosive events. This correlates well with the difference in the peak acoustic pressure between each explosive event; the peak pressure was 151 Pa during the 23 March 07:02 event and only 49 Pa during the 29 March 03:24 event. The rates of regular flashes, small discharges and single-source discharges dramatically increased at 03:28, which coincided with the approximate end of the explosive activity and the beginning of the plume phase.

A third example of the evolution of lightning rates comes from the 23 March 08:14 volcanic lightning storm and is an example of a storm with a long duration explosive event. In this case, shown in Fig. 15, we still saw higher rates of small discharges and single source discharges than regular flashes early on in the explosive phase, but regular flash rates increased before the explosive eruption had ended. This was typical behavior for long duration explosive events and was due to the plume phase lightning overlapping with the explosive phase.

Once an explosive eruption had ended and the lightning transitioned to being predominantly plume phase activity, we typically observed decreasing discharge rates concurrent with increasing discharge area over the course of the rest of the storm. During the 29 March 03:24 storm plume phase activity was highest between 03:29 and 03:35, as shown by Fig. 14. During this period the peak rates were approximately 100/min for regular flashes, 110/min for small discharges and roughly 1500/min for single-source discharges. While the rates were at their peak, the average area of the regular flashes was relatively small (2–3 km²), as shown in Fig. 16. Moreover, all of the discharges that occurred during the time of peak discharge rates were relatively small due to the fact that small discharges and single-source discharges are small discharges by definition. Between 03:36 and 03:37 the flash rates declined to 20/min for regular flashes, 5/min for small discharges and less than 50/min for single-source

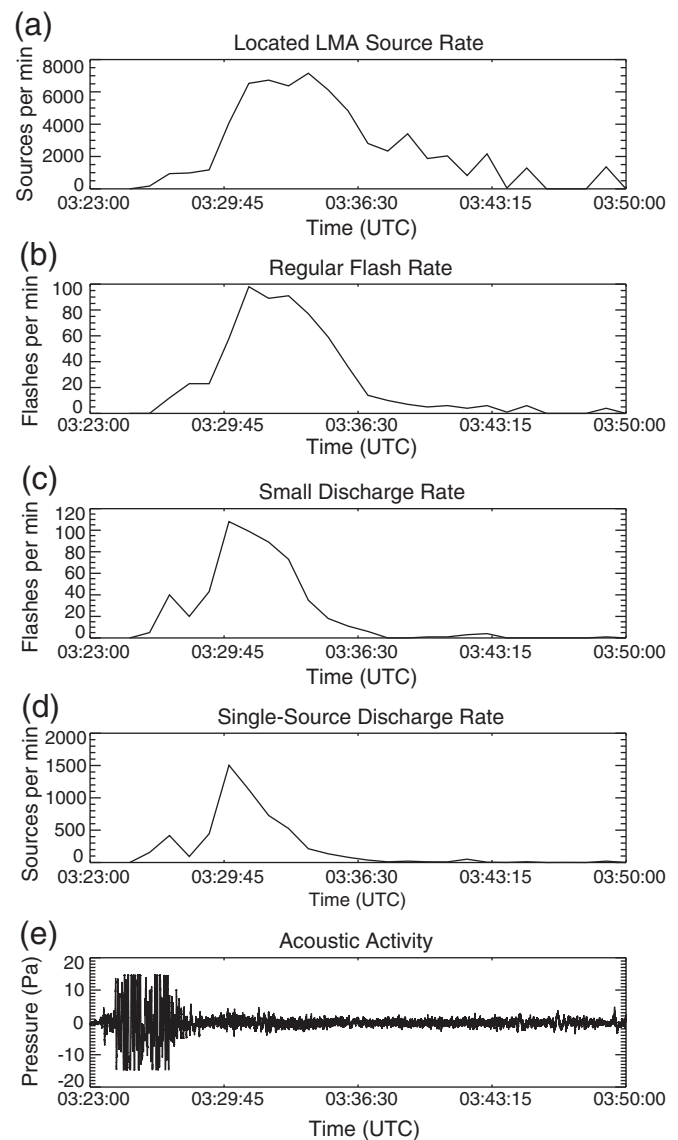


Fig. 14. The rate of total located LMA sources (panel a), regular flashes (panel b), small discharges (panel c), and single-source discharges (panel d), and the acoustic activity (panel e) during the volcanic lightning storm on 29 March at 03:24 UTC. The acoustic signal has been time-shifted to account for the travel time delay.

discharges. At this time the area of regular flashes began to increase significantly and reached a peak of 11 km² between 03:37 and 03:38. The regular flash rate remained more or less constant throughout the rest of the storm and very few single-source discharges and small discharges were observed after 03:37. The trend of increasing discharge area at the same time as decreasing discharge rate is common to the plume phase of all the volcanic lightning storms, with maximum flash areas for all storms ranging between 10 and 50 km².

3.2.2. Plume charge structure

Without the altitudes of the sources, we weren't able to infer the details of the plumes' charge structures, but the sizes and types of discharges that occurred in the plume phases do reveal that the charge structure evolved from an initially chaotic structure consisting of groups of charge spread throughout the plume to a horizontally stratified structure similar to thunderstorms (for background on thunderstorm lightning and charge structure, see MacGorman and Rust, 1998). During the 29 March 03:24 storm, high rates of located LMA sources were observed between 03:29 and 03:35. In this period, the regular flash rate reached its peak and the average area of the regular

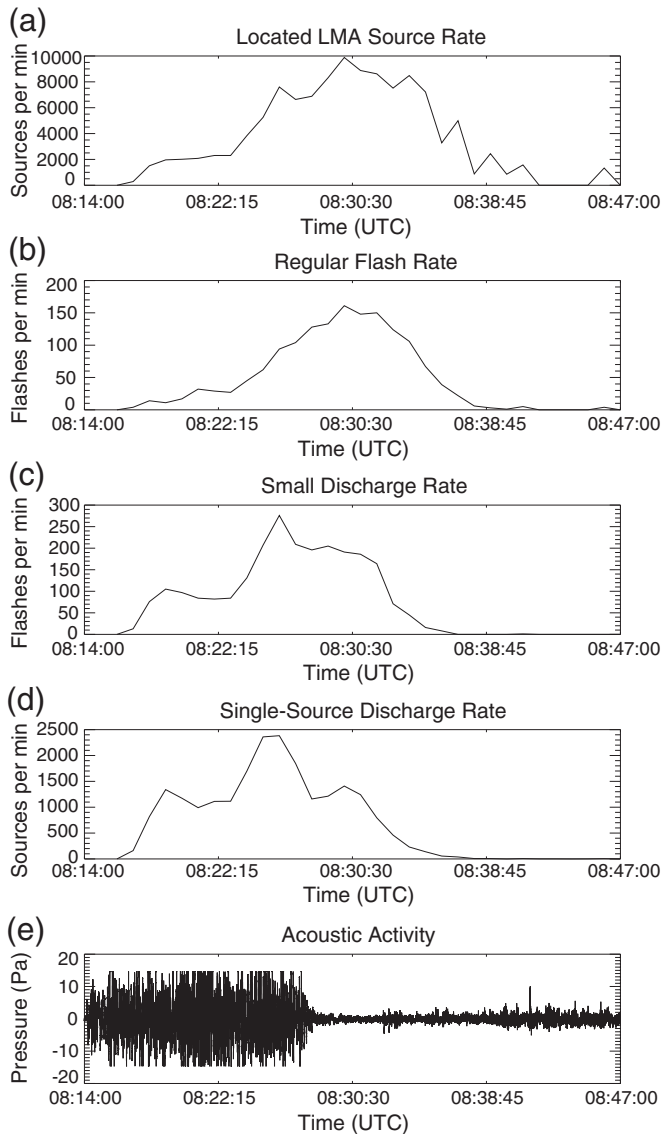


Fig. 15. The rate of total located LMA sources (panel a), regular flashes (panel b), small discharges (panel c), and single-source discharges (panel d), and the acoustic activity (panel e) during the volcanic lightning storm on 23 March at 08:14 UTC. The acoustic signal has been time-shifted to account for the travel time delay.

flashes was no more than 3 km², as shown in Fig. 16. At the same time, the rates of small discharges and single-source discharges were declining but were still occurring at relatively high rates. The small average area of regular flashes and the prevalence of large amounts of single-source discharges and small discharges at this early stage of the plume phase were a sign that the charge structure in the plume was very disorganized, clumpy and was probably constantly overturning in convective eddies at the beginning of a storm. Similar observations of complex charge structures have been observed in supercell thunderstorms (Krehbiel et al., 2000; Wiens et al., 2005; Weiss et al., 2008). The convective turmoil in the plume would prevent stratification of the large charge layers that are needed for extensive intracloud lightning flashes commonly observed in thunderstorms (Coleman et al., 2003). As the rate of regular flashes, small discharges and single-source discharges declined during the 29 March 03:24 storm, as shown in Fig. 14, the average flash area increased, shown in Fig. 16. The increase in the area of regular flashes and decline of small discharges and single-source discharges over time indicated that convective motions had subsided and stratified

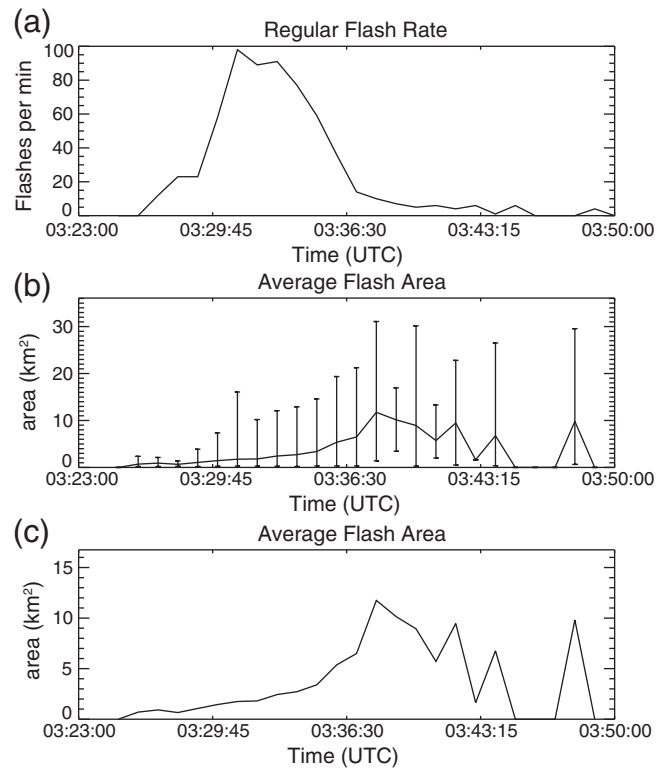


Fig. 16. The rate and average area per minute of regular flashes during the volcanic lightning storm on 29 March at 03:24 UTC. The bars in panel (b) indicate the minimum and maximum flash area in each minute. Panel (c) shows the flash area without the bars and is on a slightly expanded scale. The apparent gap in the data near the end of each panel is because no lightning was detected at that time.

charge layers had developed over time. The large flashes at the end of the storms signaled that charge layers had become very extensive.

Our results imply that, regardless of the mechanism of charge generation, gravitational settling of charged particles leads to a stratified charge structure, similar to previous studies (Lane and Gilbert, 1992; Miura et al., 2002) of the gross charge structure of small volcanic plumes from Sakurajima volcano in Japan, which revealed dipole and tripole charge structures similar to the gross charge structure of thunderstorms (Williams, 1989). Lane and Gilbert (1992) and Miura et al. (2002) measured the potential gradient beneath ash plumes at Sakurajima and determined that gravitational separation was responsible for separating oppositely charged particles that were charged during the eruption process. The Redoubt Volcano and Sakurajima measurements differ in terms of column height and charge generation mechanism, however; Redoubt Volcano's plumes were much higher and ice was likely responsible for much of the charge generation. Despite these differences, both Sakurajima results are consistent with the Redoubt Volcano and Augustine Volcano (Thomas et al., 2010) results that stratified layers develop over time due to gravitational separation.

3.3. Altitudes of discharges during the explosive phase

Even though we weren't able to locate the altitudes of the lightning discharges from the time-of-arrival processing methods, we have been able to compare our locations to radar data and put a range on the altitudes of some of the discharges that occurred during the explosive phase.

In almost every volcanic lightning storm, we observed single-source discharges directly over the vent of Redoubt Volcano while the explosive eruption, and thus the explosive phase, was going on. Oftentimes single-source discharges were the only types of

discharges that occurred during the explosive phase. Fig. 17 shows the rates of total located LMA sources and single-source discharges during the storm at 03:24 on 28 March. There were a small amount of sources observed while the acoustic signal was saturated on the high-gain channel. Except for one lightning discharge at the beginning of the event, all of the located LMA sources that were observed during this time were single-source discharges. The initial spike of located LMA sources shown in Fig. 17 (goes off scale) is from the initial flash. Single-source discharges were also observed after the acoustic signal returned to background levels, but these sources were associated with the plume phase. As shown in Fig. 18, the single-source discharges that occurred during the explosive phase occurred directly over the volcano. Most of the discharges occurred within a 1.5 km radius of Redoubt Volcano, and all were within a 5 km radius of Redoubt Volcano. Single-source discharges were commonly observed directly over Redoubt Volcano during the explosive phase in the other volcanic lightning storms.

Radar data from this explosive event showed that the altitude of the eruption column was approximately 4 km ASL when the first group of single-source discharges occurred, which indicates that the single-source discharges were occurring at or below this altitude. The eruption column first showed up on the radar during the scan starting at 03:25:44 in the 2.5 degree elevation angle sweep, and the initial group of single-source discharges were observed between 03:25:06 and 03:25:52. At a range of 82 km (approximate distance to Redoubt Volcano) an elevation angle of 2.5° corresponds to 4 km altitude. Fig. 19 shows the reflectivity scan for this sweep. The eruption column was not detected at higher elevation angles until the following scan. The single-source discharges most likely occurred within the column at or below 4 km (the summit of Redoubt Volcano is approximately 3.1 km ASL), which validates the observation made by Thomas et al. (2010) that the discharges responsible for the continual

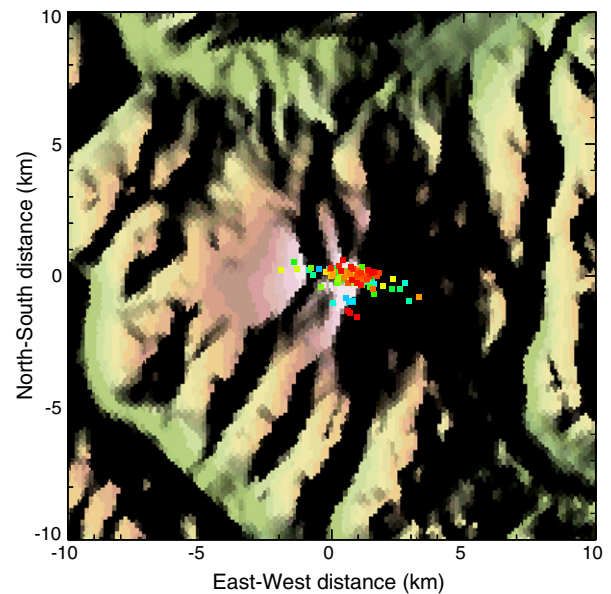


Fig. 18. Map view depiction of the single-source discharges that occurred between 03:25:06 and 03:25:52, during the explosive phase (event 13) of the volcanic lightning storm on 28 March at 03:24 UTC. The colors of the points indicate the progression of time, blue being earlier times and red later times.

RF (explosive phase) signal occurred immediately above the volcano in the eruption column.

3.4. Types of lightning discharges

Thomas et al. (2010) identified three types of discharges that occurred during the 2006 eruption of Augustine Volcano: vent discharges, near-vent lightning, and plume lightning. Vent discharges were small (on the order of 10–100 m), high rate discharges occurring directly above the vent in the eruption column. These discharges were responsible for the continual RF signal of the explosive phase. Near-vent lightning referred to discharges that were presumed to extend upward from the volcano into the eruption column, and could be 1 to 7 km in length and were also explosive phase discharges. Plume lightning described the larger lightning discharges (10 km or more) that occurred in the plume above and away from the volcano, and were thought to be similar to intracloud lightning common to thunderstorms.

Vent discharges, near-vent lightning, and plume lightning were also observed at Redoubt Volcano. The single-source discharges discussed in Section 3.3 were identified as vent discharges because they occurred during explosive events and were at low altitude. Small discharges that occurred during the explosive eruption were either larger vent discharges or small near-vent lightning. The single-source discharges and small discharges that occurred after the explosive eruption in the plume phase were likely occurring throughout the height of the eruption column, and thus qualified as small plume lightning and were the result of plume-based charge mechanisms. The majority of discharges classified as regular flashes during the plume phase also qualified as plume lightning. The LMA observations indicate that plume lightning often had large horizontal extents, similar to intracloud lightning, though photographs (B. Higgman, pers. comm.) of plume lightning early in the storms show discharges with large vertical extents as well. The explosive phase lightning observed during the weak electrical events was near-vent lightning, and the few plume phase discharges observed were plume lightning.

In addition to these three classifications of discharges, cloud-to-ground lightning was detected by the WWLLN and BLM networks.

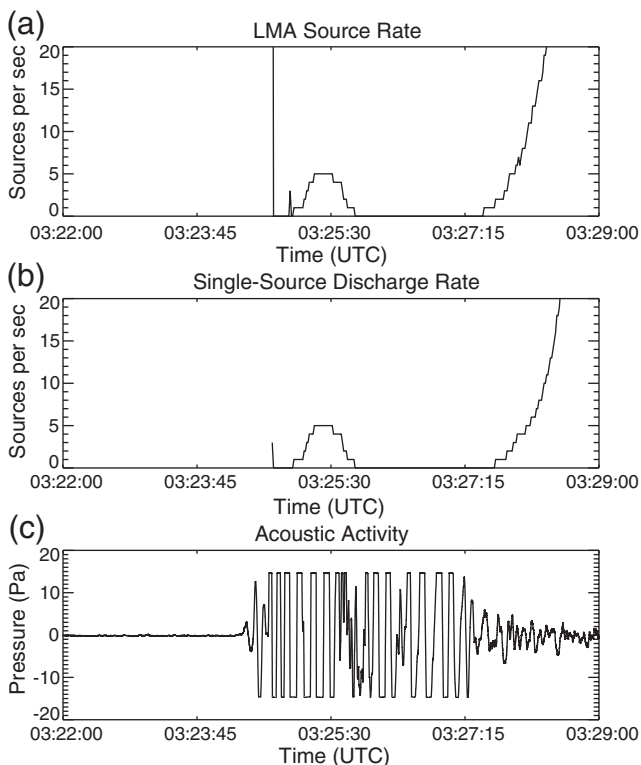


Fig. 17. Total located LMA source rate, single-source discharge rate, and acoustic activity from the volcanic lightning storm on 28 March at 03:24 UTC. The acoustic signal has been time-shifted to account for the travel time delay. The scales on the x and y axis have been expanded to emphasize the electrical activity that occurred during explosive event 13.

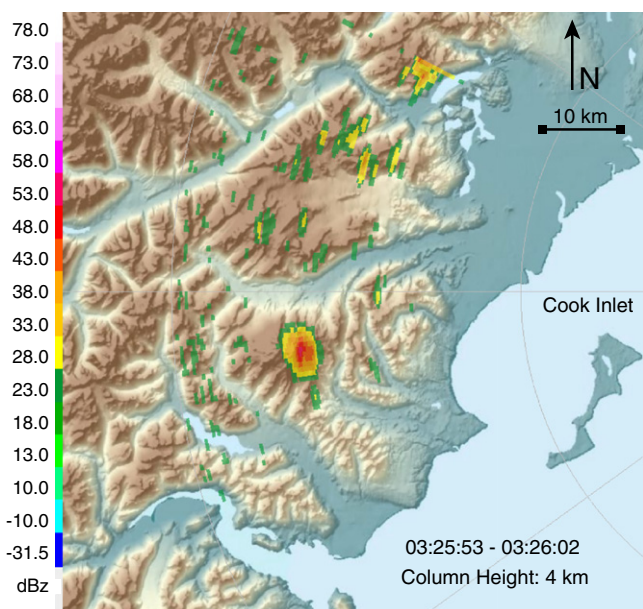


Fig. 19. Plot of the corrected reflectivity for the 2.5 degree elevation angle scan. This scan took place between approximately 03:25:53 and 03:26:02 UTC on 28 March 2009.

The cloud-to-ground lightning was observed during the plume phase and would likely have been classified by the flash algorithm as regular flashes. Because we don't know the altitudes of the located LMA sources we can't make the distinction between plume lightning and cloud-to-ground lightning with the flash algorithm.

3.5. Comparison of electrical and eruptive activity

In this section we compare the total amount of electrical activity to several measures of the eruptive activity, including peak column heights, peak acoustic pressures and durations, seismic durations, and reduced displacement (Table 1). The total number of located LMA sources is used as a measure of the total amount of electrical activity in a storm. In Figs. 20–22, the symbols referring to 4 of the events are marked in red. These 4 events produced volcanic lightning storms and during each of these storms another explosive event occurred while vigorous electrical activity was already occurring. These subsequent, or 'secondary,' events are identified in Table 1. In two cases (23 March 09:48 and 4 April 13:57) the second event was large enough to have contributed to the lightning production, but because a volcanic lightning storm was already occurring, we can't separate the lightning data between the two explosive events. In the two other cases (23 March 12:30 and 27 March 08:28) the second explosive event was small, and may have had very little or no influence on the

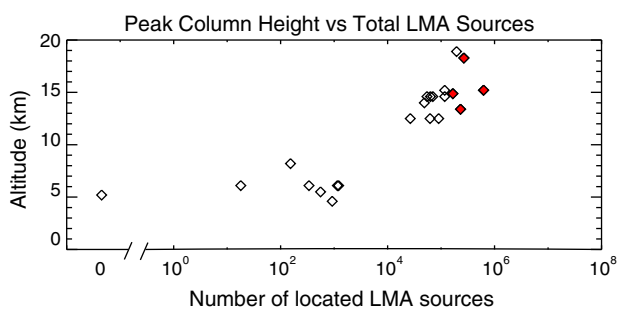


Fig. 20. Peak column height versus total number of located LMA sources for distinct explosive events during the 2009 Redoubt Volcano eruption. The red diamonds indicate events that had secondary explosive events while a volcanic lightning storm was still ongoing following the first event.

lightning. In Figs. 20–22, the data given with the red diamonds are the measurements (column height, acoustic pressure, etc.) for the first explosive event. Additionally, there are two large explosive events (24 March 03:40 and 27 March 16:39 UTC) that were excluded from Figs. 20–22. They were excluded because only 3 of the 4 stations were operating during these events due to power issues and the quantity of located LMA sources for 3-station locations cannot be fairly compared to the 4-station locations.

3.5.1. Eruption column heights

Comparison of the peak column height to the total number of LMA sources located for each explosive event showed that the volcanic lightning storms occurred in plumes with peak column heights greater than 10 km. The relationship between column height and total lightning is shown in Fig. 20. All of the volcanic lightning storms had more than 10,000 located LMA sources and occurred in eruption columns with peak altitudes greater than 10 km. Among these events we generally saw that the higher in altitude the column reached, the more lightning there was. All of the weak electrical events had less than 10,000 located sources and occurred in eruption columns with peak altitude less than 10 km. Additionally, there were several small events that had no lightning, but a column height measurement was only available for one of these events, which was also less than 10 km.

3.5.2. Acoustic activity

Analysis of the acoustic and lightning data revealed that all of the volcanic lightning storms occurred when the peak pressure was greater than 30 Pa, as shown in Fig. 21. Events without lightning and weak electrical events all occurred when the peak pressure was less than 30 Pa. Among the events with peak pressure greater than 30 Pa, there was no correlation between the peak pressure and the total number of located LMA sources. All types of activity (no lightning, weak electrical events, and volcanic lightning storms) were observed when the acoustic signal durations were less than 5 min. With a few exceptions, events with durations longer than 5 min all produced a volcanic lightning storm. There were two events with durations longer than 5 min that instead produced a weak electrical

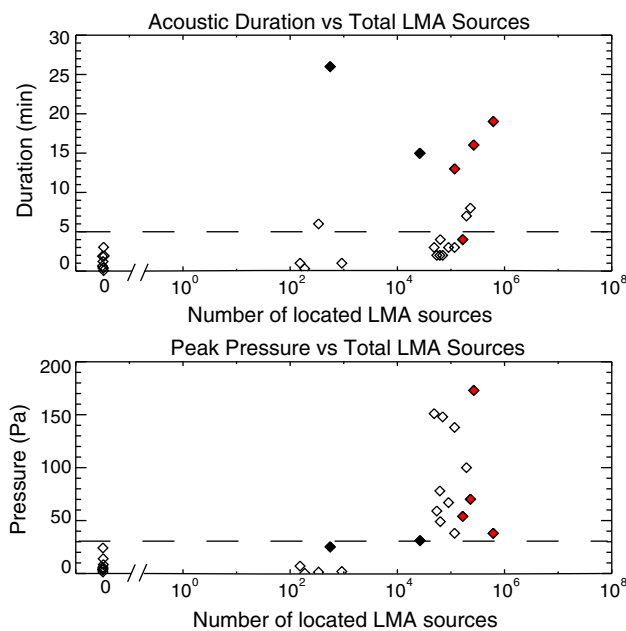


Fig. 21. Acoustic duration and peak pressure versus total located LMA sources for distinct explosive events during the 2009 Redoubt Volcano eruption. The red diamonds indicate events that had secondary explosive events while a volcanic lightning storm was still ongoing following the first event. The black diamonds indicate events with a 'pulsed' waveform (see text).

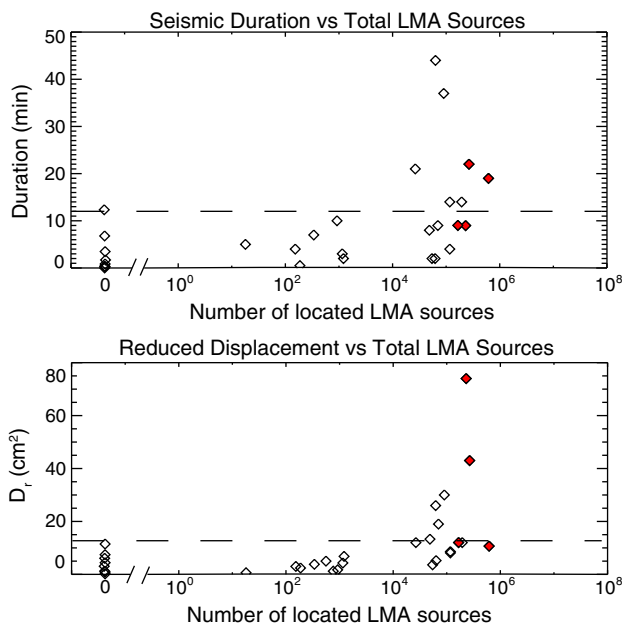


Fig. 22. Seismic duration and reduced displacement vs total located LMA sources for distinct explosive events during the 2009 Redoubt Volcano eruption. The red diamonds indicate events that had secondary explosive events while a volcanic lightning storm was still ongoing following the first event.

event. One of those was 6 min long but had a peak pressure of only 1.3 Pa (31 March 07:31). The other event was 26 min long, but the signal pulsed over that time period (it did not keep a high amplitude over the whole duration), and reached a peak amplitude of only 25 Pa. Because of the pulsating nature of the signal, we have marked this event (23 March 06:35; event 1, which produced very little ash) and a similar event with a pulsed waveform (27 March 07:47) with a black diamond in Fig. 21.

3.5.3. Seismic activity

Comparison of the total amount of lightning to the reduced displacement and seismic durations for each explosive event demonstrated that events with either long duration (greater than 12 min) or large reduced displacements (greater than 13 cm²) produced volcanic lightning storms, though storms also occurred as a result of events with shorter durations and smaller reduced displacements. Fig. 22 shows the relationship between the duration of the seismic signals and reduced displacement for each explosive event and the total number of located LMA sources. All types of activity (no lightning, weak electrical events, and volcanic lightning storms) were observed when the seismic durations were less than 12 min. Events with durations longer than 12 min produced volcanic lightning storms. Similarly, all types of activity were observed during events with reduced displacements less than 13 cm², while events with reduced displacements greater than 13 cm² produced volcanic lightning storms. Among the events with either long duration or large reduced displacement there is no correlation between the duration or reduced displacement and the total number of located LMA sources.

3.5.4. The relationship between eruptive activity and plume electrification

A significant unknown in volcanic lightning research is the degree to which plume electrification processes are controlled by water-based charging mechanisms or by the separation of charged ash. Previous research has shown that volcanic plumes contain an abundant amount of water (Sparks et al., 1997), which is in excess of thunderstorms (Williams and McNutt, 2005), and charged ash is believed to be responsible for at least the explosive phase lightning. The possible

plume charging methods were previously explored by Thomas et al. (2010). If water-based charging mechanisms are dominant, factors important for ice production and collisions should be observed to influence the total amount of lightning in a volcanic lightning storm. If ash charging mechanisms are dominant, there should be a relationship between the properties and quantity of erupted ash and the total amount of lightning.

The above results show that column height had the strongest correlation to lightning production, while there was a weak association between acoustic activity and lightning and an even weaker link between seismic activity and lightning. The relationships between acoustic activity and lightning suggest a connection between the gas released and lightning, but further study is needed to understand this connection. The amount and temporal distribution of gas released during an eruption could affect the explosivity of an eruption; higher explosivity results in finer ash and thus more charge carriers, which should result in an increase in overall electrical activity. In terms of the seismic activity, reduced displacement has been correlated to volcano explosivity index (VEI) and ash column height (McNutt, 1994), however some of the largest sources of uncertainty in these relationships came from eruptions with column heights between 10 and 20 km and with VEI of 3, which is the range consistent with the Redoubt Volcano observations. The correlation between column height and lightning is the most revealing, and supports the idea that volcanic thunderstorms become electrified in a similar manner to meteorological thunderstorms, via ice-charging mechanisms (Williams and McNutt, 2005; James et al., 2008).

There are two factors related to column height that could contribute to ice-charging mechanisms: the ambient atmospheric temperature and the thermal input from the eruption. First, the temperature in the troposphere generally decreases with altitude, so higher column altitudes would favor ice production. Laboratory results have shown that ice production on silicic particles occurs when the ambient temperature is between -10 and -20 °C (Durant et al., 2008). National Weather Service atmospheric soundings from Anchorage (retrievable from: <http://weather.uwyo.edu/upperair/sounding.html>) indicate that during the two week eruption the atmosphere was typically -20 °C or colder at altitudes of 3.5 km and above, and was at least -50 °C above altitudes of 10 km. Modeling of eruption columns (see Fig. 4.4 of Sparks et al., 1997) indicate that plume temperatures initially decline rapidly with increasing altitude, and then decrease more gradually until reaching atmospheric temperature at the level of neutral buoyancy. As given by the Sparks et al. (1997) model for a typical eruption column, a plume with peak column height of 12 km has a roughly 10–15 degree temperature difference at 9 km altitude, 3 km below the top of the column. Given ambient atmospheric temperatures of -50 °C in Alaska at 9 km, the corresponding modeled plume temperature would be between -35 and -40 °C, which is cold enough for ice production. The smaller, 6–8 km plumes observed during the Redoubt Volcano eruption would have temperatures of -35 °C (for 6 km) and -45 °C (for 8 km) at the level of neutral buoyancy, and we expect that freezing conditions would also be present within the column at altitudes 1 or 2 km below the top of the column. Second, peak column height has been related to the amount of thermal energy input during an eruption (Sparks et al., 1997), meaning that higher altitude columns should have more thermal energy, which should, in turn, create faster updrafts (column height is also affected by the stratification of the atmosphere and the height of the tropopause; the soundings also show that there were diurnal and day-to-day variations in the height of the tropopause, which was less than 10 km). In a regular thunderstorm, strong updrafts aid electrification by the condensation of water for hydrometeor growth and through an increase in collisions between graupel and ice crystals by keeping graupel particles aloft in a cloud (MacGorman and Rust, 1998).

The ambient temperature during the eruption of Redoubt Volcano was certainly cold enough to support ice production, even at altitudes

between 3.5 and 10 km, therefore it is possible that the difference between the weak electrical events or the events with no lightning and the volcanic lightning storms was the variation in updraft strength. Even after ice creation is thermodynamically possible in a plume, sufficient collisions must occur between particles of different size in order to charge the particles, which then must be sufficiently separated from each other to create strong electric fields. In the weak electrical events the updrafts may not have been strong enough or did not last long enough to create and separate a large amount of charged particles. Because there is little distinction between the weak events and the events with no lightning in terms of the seismic and acoustic activity or the column height (though there is only one plume height measurement for the no-lightning events), there is not a clear indication of why some of the small plumes did not become electrified enough to produce lightning. The ambient atmospheric conditions do not seem to have contributed to the production or non-production of lightning in the small plumes since the -20°C isotherm varied between only 2.6 and 3.7 km between 23 March and 5 April (with the exception of one spike to 4.7 km on 26 March).

If charged ash was affecting the electrification, we would expect to see a relationship between the amount of ash and the total amount of lightning from each explosive event. Though the ash deposits from the eruption were measured (Wallace et al., *this issue*), distinct measurements for every single explosive event were not possible because several of the explosive events happened in quick succession and left a composite layer of ash. Without distinct measurements for each individual event, we can't compare the amount of lightning in each volcanic lightning storm to the total amount of ash. But even if we could, the role that ash played in electrification would still be unclear because ash could contribute to electrification in multiple ways. First, because the ash was already charged, it could have added to the electrification of the plume simply through gravitational separation of ash of opposite polarities. But ash and ice were not necessarily separate particles in the plume. Ash can act as condensation and/or ice nuclei, so the charged ash could have become ice particles, which would have then acquired a greater or lesser charge through collisions with other ice particles. Therefore, ash and water-based electrification mechanisms may have been working together in the plume, and aren't necessarily separable from each other.

A similar correlation between column height and lightning was observed by Bennett et al. (2010) during the eruption of Eyjafjallajökull, however due to differences in the types of lightning measured and the types of eruptions between Redoubt Volcano and Eyjafjallajökull, a detailed comparison between both sets of results is not appropriate. Bennett et al. (2010) compared lightning rates detected by the UK Met Office ATDnet (a long-range lightning location network that detects return strokes from cloud-to-ground lightning with a peak current greater than 3 kA) and found that during times when the plume produced lightning, there was a linear correlation between column height and the number of detected lightning strokes (there were conflicting times when elevated column heights did not produce lightning and Bennett et al. (2010) noted that ambient atmospheric conditions could have played a role in this). Cloud-to-ground lightning is, however, not necessarily the best measure of total electrical activity. In the Redoubt Volcano data, for example, there is not a linear relationship between the number of regular flashes in a storm and the number of cloud-to-ground discharges detected by either the WLLN or BLM networks. Nevertheless, in the larger picture these results are further evidence that factors related to plume height are playing a role in lightning production in volcanic plumes.

4. Conclusions

The electrical activity observed during the explosive events of the 2009 Redoubt Volcano eruption was very similar to the electrical

activity observed during the 2006 eruption of Augustine Volcano. The explosive and plume phases of electrical activity first observed at Augustine Volcano were also observed during Redoubt Volcano's volcanic lightning storms. Similar to Augustine Volcano, explosive phase activity at Redoubt Volcano consisted of vent discharges and near-vent lightning that were identified using the flash algorithm as single-source discharges and small discharges. Plume phase activity at Redoubt Volcano was much more intense than what was observed at Augustine Volcano (the explosive eruptions of Redoubt Volcano were also much larger than Augustine Volcano); a few hundred discharges were observed during the plume phase of an explosive event at Augustine Volcano, while thousands of discharges were observed during the plume phases of the volcanic lightning storms at Redoubt Volcano. Plume lightning at Augustine Volcano consisted of thunderstorm-like discharges that were 10 km or more in length, while plume lightning at Redoubt Volcano varied greatly in size and included the roughly 100-meter single-source discharges and extensive regular flashes up to 50 km² in area and 20 km or more in length.

The Redoubt Volcano results support the Augustine Volcano findings that two separate electrification mechanisms were responsible for the two observed regimes of electrical activity, namely an explosion-based charging mechanism and a plume-based charging mechanism. Despite the observed delay in the onset of the continual RF (explosive phase) signal during the explosive eruptions at Redoubt Volcano, the signal was still correlated with the explosive activity and was likely also caused by an explosion based charging mechanism such as fractoemission and the boiling of water. The difference in the relative strength of the continual RF signal between Redoubt Volcano (Redoubt Volcano being less strong) and Augustine Volcano was probably due to the eastern ridge of Redoubt Volcano blocking the view of the activity. Additionally, even though there was no lull observed between the explosive and plume phases at Redoubt Volcano, the time between the onset of the eruption and the onset of the plume phase is sufficiently long to account for the time needed for water-based or ash-based electrification of the plume phase. This difference and the difference in the amount of plume lightning between Augustine Volcano and Redoubt Volcano is most likely due to Redoubt Volcano's explosive events being much larger and more energetic. Background atmospheric conditions can play a significant role in ice creation and thus electrification, but the size of the explosive events is the dominant factor here. The observations of lightning from Redoubt Volcano support the findings from Augustine Volcano that the explosive phase was the result of charged ash electrified by eruptive mechanisms and that the plume phase was the result of subsequent and likely water-based electrification processes in the plume.

Our lightning observations show that the charge structure of the plume evolved over the duration of a storm from an initially disorganized and clumpy structure to a horizontally stratified structure similar to what is observed in meteorological thunderstorms. Lightning during the early stages of the plume phase consisted of high rates of single-source discharges, small discharges, and high rates of regular flashes that were on average no larger than 3 km². This indicates that the charge structure was initially chaotic and most likely consisted of clumps of positive and negative charge strewn throughout the initially turbulent plume. Over time, discharge rates decreased and the area of regular flashes increased, indicating that turbulence was subsiding and stratified charge layers similar to those in thunderstorms were developing.

The overall size of a volcanic lightning storm, as measured by the total number of located LMA sources, was most strongly influenced by the peak height of the eruption column. The volcanic lightning storms occurred in plumes with peak column heights greater than 10 km and the weak electrical events and events with no lightning occurred in plumes with peak column heights less than 10 km. It is possible that the thermal energy responsible for the eruption columns greater than 10 km created strong updrafts, providing similar

conditions prevalent in thunderstorms for strong electrification through the collisions of ice particles. The eruption columns less than 10 km may not have had updrafts with the strength and duration needed to create and separate a sufficient amount of charged ice particles.

The frequent occurrence of lightning during the eruption of Redoubt Volcano reinforced just how common lightning is in volcanic eruptions, and showed that lightning is an indicator of explosive volcanic activity and is useful for volcano monitoring. If the LMA was used in monitoring situations, observations of the explosive phase VHF signal could be used to confirm or detect explosive activity because it is unique to volcanic eruptions, unlike the discrete VHF signal produced by plume phase lightning. The origin (volcanic or meteorological) of plume phase lightning, especially in situations where no explosive phase is detected, could be ambiguous because of its similarities with meteorological lightning. The LMA could be particularly useful for monitoring volcanoes in remote locations where visual observations are scarce, and at high latitudes where thunderstorms are rare.

Acknowledgments

We recognize the contributions made by Sandra Kieft and Graydon Aulich of New Mexico Tech, and Edward Clark of the Alaska Volcano Observatory. We thank the individuals and organizations who hosted our instruments in Alaska, and the individuals with the Kenai Peninsula Borough who provided on site technical support to one of our stations. We appreciate the contributions of lightning data by Thor Weatherby, of the Alaska BLM, and by the World Wide Lightning Location Network. This work was supported by the National Science Foundation under grant ATM-0739085.

Appendix A. The flash algorithm

A flash algorithm was used to sort the located LMA sources into distinct flashes. The goal was to design a flash algorithm that could accommodate a range of discharge size from less than 100 m to a few tens of km in length and a rate of up to many hundreds of sources per second, like the examples shown in Figs. 23 and 24. Each of these plots show the y (north–south) position of the located sources vs time. The colors indicate groups of sources that were qualified to be flashes according to the requirements of the flash algorithm and the black points are sources that did not meet the criteria for being part

of a flash, though the majority of the sources are real signals from lightning discharges of various sizes (a small amount of the sources are noise). During times of relatively high rate activity (e.g. Fig. 23a) the distribution of sources in space and time was much more homogeneous than during times of low rate activity (e.g. Fig. 23b and 24a), making it very difficult to determine how the sources should be grouped into flashes. Some of the larger groups of colored points in Fig. 23a stand out as obvious flashes, but there are many scattered single sources that do not appear to be associated with other sources. It is important to reiterate that all of the sources in Figs. 23 and 24 are real signals from lightning discharges, even the scattered single sources, which are just very small discharges.

The difficulty with designing the algorithm was that the parameters for separation in space and time between points that would correctly group all of the sources in Fig. 24b into one flash would incorrectly group sources during times of high rate activity. There were gaps in time and space of up to 50 ms and 1.5 km between the channels of the discharge in Fig. 24b. If the algorithm tried to group the sources in Fig. 23a into flashes by limiting the separation between points to no more than 50 ms in time and 1.5 km in space, the algorithm would have grouped the entire 20 s into a handful of multi-second long discharges, which would be obviously incorrect. Thus the challenge in designing the flash algorithm was to find parameters that could identify flashes in both of the situations that Figs. 23 and 24 present.

The flash algorithm used on the Redoubt Volcano data set works by searching for clusters of points and then combines the clusters into flashes while making two passes through the data. On the first pass the allowed separation in time and space between sources is small enough that the previously mentioned scattered single sources won't be grouped with other single points or with other clusters. Clusters of at least three or more points move on to the second pass. Any other points, including points that were not near enough to others to form a cluster, are marked as 'single-source discharges' and are excluded from the second pass. The second pass uses a time and space separation that is large enough to group clusters into flashes like those shown in Fig. 24. The flashes identified in the second pass are divided into two categories: 'regular flashes' (clusters from the second pass that have 10 or more sources), and 'small discharges' (clusters from the second pass that have less than 10 sources). The parameters used for this paper were 500 m and 10 ms for the first

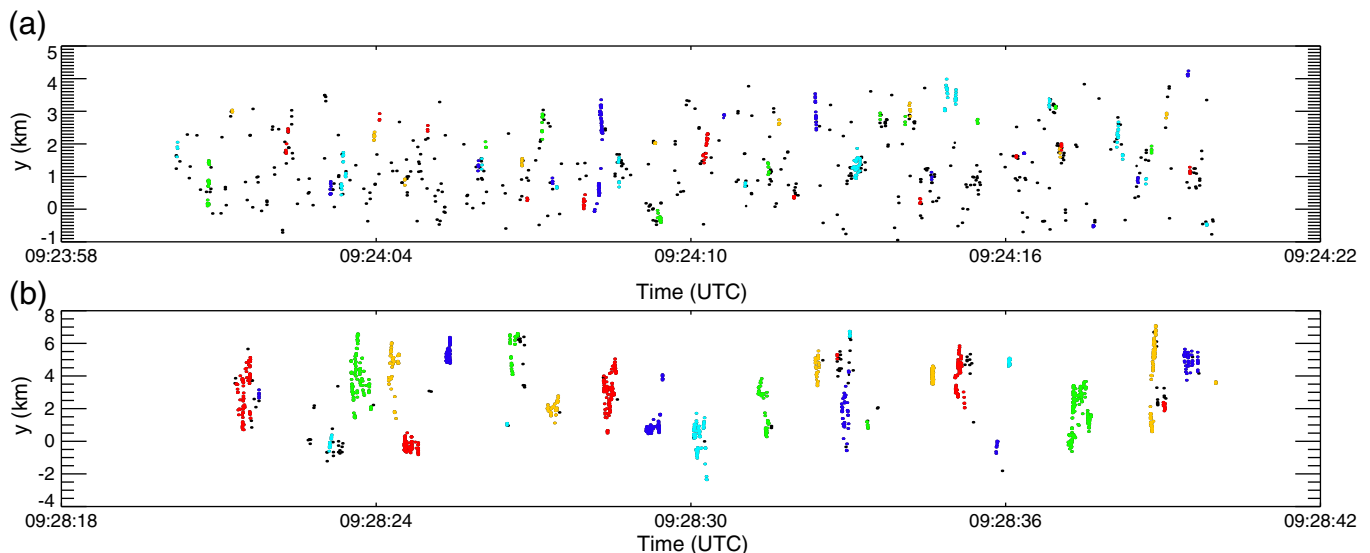


Fig. 23. Two examples of located LMA data from 28 March, plotted as the y (north–south) position vs time. Panel (a) shows 20 s of data during a period of relatively high-rate activity, while panel (b) shows 20 s of data during a period of relatively low-rate activity. The colors indicate groups of points that were identified as flashes or small discharges by the flash algorithm. The black points are sources identified as single-source discharges.

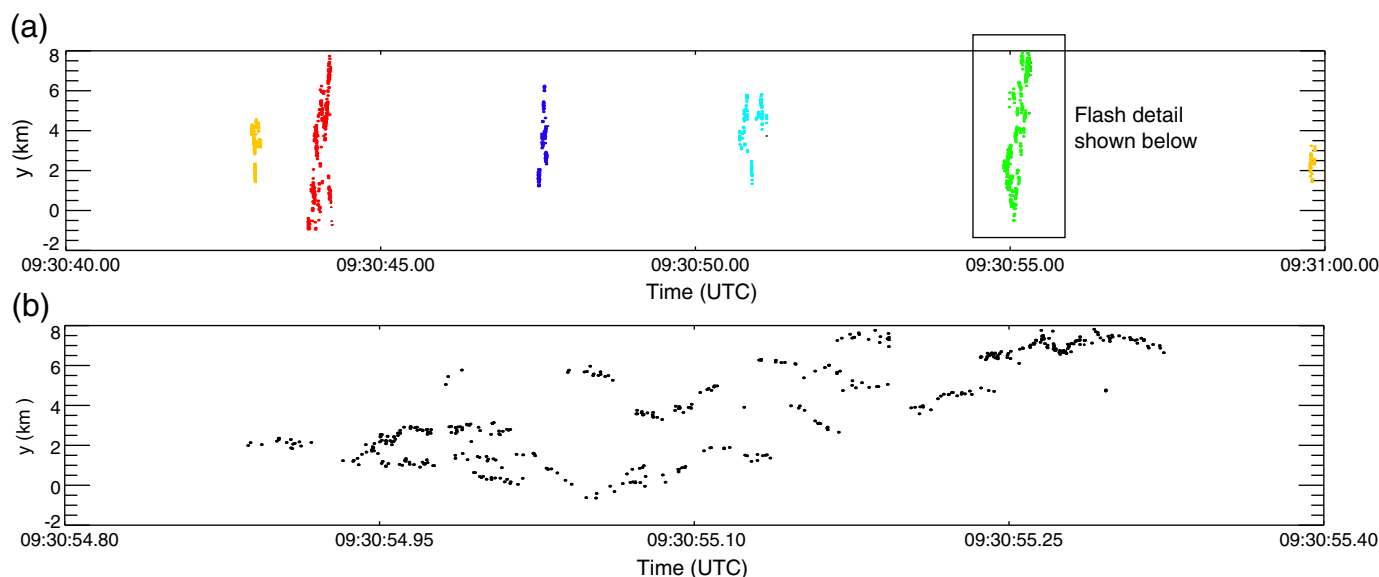


Fig. 24. An example of relatively large intracloud lightning on 28 March, plotted as the y (north–south) position vs time. Panel (b) shows one of the large discharges from panel (a) on an expanded time scale.

pass and 2500 m and 150 ms for the second pass. These parameters are more restrictive than those reported by MacGorman et al. (2008), who used a space and time separation of 3000 m and 500 ms for thunderstorm studies.

After the algorithm classifies the flashes, the area of each discharge is also determined. To calculate the area of a discharge, each flash was superimposed on a uniform grid in x and y . A grid size of 200 m by 200 m was used to take into account the uncertainty of the x and y locations. The total number of grid squares that each flash encompassed was counted and then multiplied by the area of one grid square (0.04 km^2).

The decision to use 10 sources as a defining line between a regular flash and a small discharge was somewhat arbitrary, but was done to separate groups of points that had more developed structure (regular flashes) from groups of points that had less structure (small discharges). This decision is supported by the fact that small discharges all encompassed an area of less than 0.4 km^2 . There were some regular flashes that were also less than 0.4 km^2 , but because they had more sources there was more structure to the discharges and they were more similar to a regular lightning discharge than a small discharge is with 3 or 5 points. Though we are making a distinction between single-source discharges, small discharges, and regular flashes it is important to keep in mind that these classifications simply describe lightning discharges with a varying number of sources and there is really a continuous distribution of discharge size ranging from less than 100 m to many kilometers in length.

References

- Bennett, A., Odams, P., Edwards, D., Arason, P., 2010. Monitoring of lightning from the April–May 2010 Eyjafjallajökull volcanic eruption using a very low frequency lightning location network. *Environmental Research Letters* 5, 44013–44022.
- Coleman, L.M., Marshall, T.C., Stolzenberg, M., Hamlin, T., Krehbiel, P.R., Rison, W., Thomas, R.J., 2003. Effects of charge and electrostatic potential on lightning propagation. *Journal of Geophysical Research* 108, 4298. doi:10.1029/2002JD002718.
- Dowden, R.L., Brundell, J.B., Rodger, C.J., 2002. VLF lightning location by time of group arrival (TOGA) at multiple sites. *Journal of Atmospheric and Solar–Terrestrial Physics* 64, 817–830.
- Durant, A.J., Shaw, R.A., Rose, W.I., Mi, Y., Ernst, G.G.J., 2008. Ice nucleation and over-seeding of ice in volcanic clouds. *Journal of Geophysical Research* 113, D09206. doi:10.1029/2007JD009064.
- Hoblitt, R., 1994. An experiment to detect and locate lightning associated with eruptions of Redoubt Volcano. *Journal of Volcanology and Geothermal Research* 62, 499–517.

- James, M.R., Lane, S.J., Gilbert, J.S., 2000. Volcanic plume electrification – experimental investigation of fracture-charging mechanism. *Journal of Geophysical Research* 105, 16641–16649.
- James, M.R., Wilson, L., Lane, S.J., Gilbert, J.S., Mather, T.A., Harrison, R.G., Martin, R.S., 2008. Electrical charging of volcanic plumes. *Space Science Reviews* 137, 399–418.
- Krehbiel, P.R., Thomas, R.J., Rison, W., Hamlin, T., Harlin, Davis, M., 2000. GPS based mapping system reveals lightning inside storms. *Eos* 81, 21–25.
- Lane, S.J., Gilbert, J.S., 1992. Electric potential gradient changes during explosive activity at Sakurajima volcano, Japan. *Bulletin of Volcanology* 54, 590–594.
- MacGorman, D.R., Rust, W.D., 1998. *The Electrical Nature of Storms*. Oxford University Press.
- MacGorman, D.R., Rust, W., Schuur, T.J., Biggerstaff, M.I., Straka, J.M., Ziegler, C.L., Mansell, E.R., Bruning, E.C., Kuhlman, K.M., Lund, N.R., Biermann, N.S., Carey, L.D., Krehbiel, P.R., Rison, W., Eack, K.B., Beasley, W.H., 2008. TELEX: the thunderstorm electrification and lightning experiment. *Bulletin of the American Meteorological Society* 89, 997–1013.
- McNutt, S.R., 1994. Volcanic tremor amplitude correlated with eruption explosivity and its potential use in determining ash hazards to aviation. *U.S. Geological Survey Professional Paper* 2047, 377–385.
- McNutt, S.R., Davis, C., 2000. Lightning associated with the 1992 eruptions of Crater Peak Mount Spurr Volcano, Alaska. *Journal of Volcanology and Geothermal Research* 102, 45–65.
- McNutt, S.R., Williams, E., 2010. Volcanic lightning: global observations and constraints on source mechanisms. *Bulletin of Volcanology* 72, 1153–1167.
- McNutt, S.R., Tytgat, G., Estes, S.A., Stihler, S.D., 2010. A parametric study of the January 2006 explosive eruptions of Augustine Volcano, using seismic, infrasonic and lightning data. In: Powers, J., Coombs, M., Freymueller, J. (Eds.), *The 2006 Eruption of Augustine Volcano: Alaska*. U.S. Geological Survey Professional Paper 1769, pp. 86–102.
- McNutt, S.R., West, M., Fee, D., Thompson, D., Stihler, S., Clark, E., this issue. Local seismic and infrasound observations of the 2009 explosive eruptions of Redoubt Volcano, Alaska. *Journal of Volcanology and Geothermal Research, Special Issue on the 2009 Redoubt Eruption*. In review.
- Miura, T., Koyaguchi, T., Tanaka, Y., 2002. Measurements of electric charge distribution in volcanic plumes at Sakurajima Volcano, Japan. *Bulletin of Volcanology* 64, 75–93.
- Rison, W., Thomas, R.J., Krehbiel, P.R., Hamlin, T., Harlin, J., 1999. A GPS-based three-dimensional lightning mapping system – initial observations. *Geophysical Research Letters* 26, 3573–3576.
- Rodger, C.J., Brundell, J.B., Dowden, R.L., 2005. Location accuracy of VLF World Wide Lightning Location (WWLL) network: post-algorithm upgrades. *Annales Geophysicae* 23, 277–290.
- Schaefer, J., 2011. The 2009 eruption of Redoubt Volcano, Alaska: Alaska Division of Geological & Geophysical Surveys Report of Investigations, 2011–5, 45 p.
- Schneider, D., Hoblitt, R., this issue. Doppler weather radar observations of the 2009 eruption of Redoubt Volcano, Alaska. *Journal of Volcanology and Geothermal Research, Special Issue on the 2009 Redoubt Eruption*. In review.
- Sparks, R.S.J., Bursik, M.I., Carey, S.N., Gilbert, J.S., Glaze, L.S., Sigurdsson, H., Woods, A.W., 1997. *Volcanic Plumes*. John Wiley and Sons, New York. pp. 97–101.
- Thomas, R.J., Krehbiel, P.R., Rison, W., Hunyady, S., Winn, W.P., Hamlin, T., Harlin, J., 2004. Accuracy of the Lightning Mapping Array. *Journal of Geophysical Research* 109, D14207. doi:10.1029/2004JD004549.
- Thomas, R.J., Krehbiel, P.R., Rison, W., Edens, H.E., Aulich, G.D., Winn, W.P., McNutt, S.R., Tytgat, G., Clark, E., 2007. Electrical activity during the 2006 Mount St. Augustine volcanic eruptions. *Science* 315, 1097.

- Thomas, R.J., McNutt, S.R., Krehbiel, P.R., Rison, W., Aulich, G., Edens, H.E., Tytgat, G., Clark, E., 2010. Lightning and electrical activity during the 2006 eruption of Augustine Volcano. In: Powers, J., Coombs, M., Freymueller, J. (Eds.), *The 2006 Eruption of Augustine Volcano: Alaska*. U.S. Geological Survey Professional Paper 1769, pp. 579–608.
- Trabant, D., Hawkins, D.B., 1997. Glacier ice volume modeling and glacier volumes on Redoubt Volcano, Alaska: U.S. Geological Survey Water Resources Investigations Report WRI 97-4187. 29 pp.
- Wallace, K., Schaefer, J., Coombs, M., this issue. Character, mass, distribution, and origin of tephra-fall deposits from the 2009 eruption of Redoubt Volcano, Alaska. *Journal of Volcanology and Geothermal Research*, Special Issue on the 2009 Redoubt Eruption. In review.
- Weiss, S.A., Rust, W.D., MacGorman, D.R., Bruning, E.C., Krehbiel, P.R., 2008. Evolving complex electrical structures of the STEPS 25 June 2000 multicell storm. *Monthly Weather Review* 136, 741–756.
- Wiens, K.C., Rutledge, S.A., Tessendorf, S.A., 2005. The 29 June 2000 supercell observed during steps. Part II: lightning and charge structure. *Journal of the Atmospheric Sciences* 62, 4151–4177.
- Williams, E.R., 1985. Large scale charge separation in thunderclouds. *Journal of Geophysical Research* 90, 6013–6025.
- Williams, E.R., 1989. The tripole structure of thunderstorms. *Journal of Geophysical Research* 94, 13151–13167.
- Williams, E.R., McNutt, S.R., 2005. Total water contents in volcanic eruption clouds and implications for electrification and lightning. In: Pontikis, C. (Ed.), *Recent Progress in Lightning Physics: Research Signpost*, pp. 81–94.